



UNIVERSITAT DE
BARCELONA

Caracterización del vulcanismo carbonatítico de Catanda (Angola)

Marc Campeny Crego

ADVERTIMENT. La consulta d'aquesta tesi queda condicionada a l'acceptació de les següents condicions d'ús: La difusió d'aquesta tesi per mitjà del servei TDX (www.tdx.cat) i a través del Dipòsit Digital de la UB (diposit.ub.edu) ha estat autoritzada pels titulars dels drets de propietat intel·lectual únicament per a usos privats emmarcats en activitats d'investigació i docència. No s'autoritza la seva reproducció amb finalitats de lucre ni la seva difusió i posada a disposició des d'un lloc aliè al servei TDX ni al Dipòsit Digital de la UB. No s'autoritza la presentació del seu contingut en una finestra o marc aliè a TDX o al Dipòsit Digital de la UB (framing). Aquesta reserva de drets afecta tant al resum de presentació de la tesi com als seus continguts. En la utilització o cita de parts de la tesi és obligat indicar el nom de la persona autora.

ADVERTENCIA. La consulta de esta tesis queda condicionada a la aceptación de las siguientes condiciones de uso: La difusión de esta tesis por medio del servicio TDR (www.tdx.cat) y a través del Repositorio Digital de la UB (diposit.ub.edu) ha sido autorizada por los titulares de los derechos de propiedad intelectual únicamente para usos privados enmarcados en actividades de investigación y docencia. No se autoriza su reproducción con finalidades de lucro ni su difusión y puesta a disposición desde un sitio ajeno al servicio TDR o al Repositorio Digital de la UB. No se autoriza la presentación de su contenido en una ventana o marco ajeno a TDR o al Repositorio Digital de la UB (framing). Esta reserva de derechos afecta tanto al resumen de presentación de la tesis como a sus contenidos. En la utilización o cita de partes de la tesis es obligado indicar el nombre de la persona autora.

WARNING. On having consulted this thesis you're accepting the following use conditions: Spreading this thesis by the TDX (www.tdx.cat) service and by the UB Digital Repository (diposit.ub.edu) has been authorized by the titular of the intellectual property rights only for private uses placed in investigation and teaching activities. Reproduction with lucrative aims is not authorized nor its spreading and availability from a site foreign to the TDX service or to the UB Digital Repository. Introducing its content in a window or frame foreign to the TDX service or to the UB Digital Repository is not authorized (framing). Those rights affect to the presentation summary of the thesis as well as to its contents. In the using or citation of parts of the thesis it's obliged to indicate the name of the author.

Publicaciones originales

9.2. Publicación II

Campany M., Kamenetsky, V.S., Melgarejo J.C., Mangas J., Manuel J., Alfonso P., Bambi A., Kamenetsky, M.B., Gonçalves, O.A. (2015): Carbonatitic lavas in Catanda (Kwanza Sul, Angola): Mineralogical and geochemical constraints on the parental melt. *Lithos* 232, 1-11.



Carbonatitic lavas in Catanda (Kwanza Sul, Angola): Mineralogical and geochemical constraints on the parental melt



Marc Campeny^a, Vadim S. Kamenetsky^b, Joan C. Melgarejo^a, José Mangas^c, José Manuel^d, Pura Alfonso^e, Maya B. Kamenetsky^b, Aurora C.J.M. Bambi^d, Antonio O. Gonçalves^d

^a Dept. Cristal·lografia, Mineralogia i Dipòsits Minerals, Universitat de Barcelona, Barcelona, Catalonia, Spain

^b School of Physical Sciences, University of Tasmania, Hobart, Australia

^c Depto. Física, Instituto de Oceanografía y Cambio Global, Universidad de Las Palmas de Gran Canaria, Spain

^d Depto. Geología, Universidade Agostinho Neto, Luanda, Angola

^e Dept. Enginyeria Minera i Recursos Naturals, Universitat Politècnica de Catalunya, Manresa, Catalonia, Spain

ARTICLE INFO

Article history:

Received 17 January 2015

Accepted 13 June 2015

Available online 4 July 2015

Keywords:

Carbonatitic lavas

Natrocarnatites

Silicocarbonatites

Angola

Catanda

ABSTRACT

A set of small volcanic edifices with tuff ring and maar morphologies occur in the Catanda area, which is the only locality with extrusive carbonatites reported in Angola. Four outcrops of carbonatite lavas have been identified in this region and considering the mineralogical, textural and compositional features, we classify them as: silicocarbonatites (1), calciocarbonatites (2) and secondary calciocarbonatites produced by the alteration of primary natrocarnatites (3). Even with their differences, we interpret these lava types as having been a single carbonatite suite related to the same parental magma. We have also estimated the composition of the parental magma from a study of melt inclusions hosted in magnetite microphenocrysts from all of these lavas. Melt inclusions revealed the presence of 13 different alkali-rich phases (e.g., nyerereite, shortite, halite and sylvite) that argues for an alkaline composition of the Catanda parental melts. Mineralogical, textural, compositional and isotopic features of some Catanda lavas are also similar to those described in altered natrocarnatite localities worldwide such as Tinderet or Kerimasi, leading to our conclusion that the formation of some Catanda calciocarbonatite lavas was related to the occurrence of natrocarnatite volcanism in this area. On the other hand, silicocarbonatite lavas, which are enriched in periclase, present very different mineralogical, compositional and isotopic features in comparison to the rest of Catanda lavas. We conclude that its formation was probably related to the decarbonation of primary dolomite bearing carbonatites.

© 2015 Elsevier B.V. All rights reserved.

1. Introduction

There are more than 500 known carbonatite localities worldwide (Woolley and Kjarsgaard, 2008). Most of these carbonatites (~90%) are formed in plutonic or hypabyssal environments, while only a minority (~10%) are extrusive and associated with volcanic eruptions (Woolley and Church, 2005). These volcanic carbonatites are mainly formed by pyroclastic materials from explosive volcanism, while effusive carbonatite lavas have only been described in 14 localities by Woolley and Church, 2005.

Carbonatite magmas most probably represent low-degree partial melts of the lithospheric mantle (Bell and Simonetti, 2010; Wallace and Green, 1988). Therefore, the study of such extrusive products, especially lavas, provides significant information about their genesis and the concentration of chemical elements in carbonatite magmas such as *Rare Earth Elements* (REE) (Chakhmouradian and Wall, 2012;

Hornig-Kjarsgaard, 1998) and *High Field Strength Elements* (HFSE) (Chakhmouradian, 2006; Dalou et al., 2009).

Even so, due to their rarity, the scientific literature about carbonatite lava localities is very limited. Petrogenetic studies have been reported for some localities, especially from the East African Rift area (Woolley, 2001) such as Fort Portal, Uganda (Barker and Nixon, 1989; Eby et al., 2009; Nixon and Hornung, 1973; von Knorring and Du Bois, 1961), Tinderet, Kenya (Deans and Roberts, 1984; Zaitsev et al., 2013) or Kerimasi and Oldoinyo Lengai in Tanzania (Church, 1996; Dawson, 1962a; Dawson et al., 1995a; Guzmics et al., 2011, 2012, 2015; Hay, 1983; Keller and Zaitsev, 2012). Oldoinyo Lengai is the only active carbonatite volcano known, and where unique natrocarnatite lavas have also been carefully studied (Bell and Keller, 1995; Dawson, 1962b; Dawson et al., 1995b; Mitchell and Kamenetsky, 2012).

In the present contribution, we report mineralogical, geochemical, stable isotopes and melt inclusion data on the carbonatite lavas from Catanda, Angola. This carbonatite locality was first reported by Silva and Pereira (1973), but the Angolan civil war hampered the access to the area and prevented more detailed studies, until Campeny et al.

E-mail address: mcampeny@ub.edu (M. Campeny).

(2014) described the volcanic processes related to the carbonatites emplacement. These relatively fresh carbonatite lavas located in the western African margin, are in a tectonic region affected by the break-up of Gondwana (Issa Filho et al., 1991), where carbonatite magmatism is also associated to kimberlite pipes (Robles-Cruz et al., 2012).

The aim of this work is to investigate these well-preserved carbonatite lavas through a detailed petrographic description and comparing their textural and mineralogical features with other carbonatite and natrocarbonatite localities worldwide. Melt inclusion study has also permitted constraints on the composition of Catanda parental melt, which has been determined as alkali-rich.

2. Geological setting

The Catanda carbonatites are located in the Kwanza Sul province (Angola), approximately 50 km SE of the town of Sumbe and 250 km south of Luanda, the national capital. They were formed by a group of relatively eroded monogenetic volcanic cones outcropping in a 50-km² graben hosted in Archean granites (Fig. 1). The volcanic edifices of Catanda have principally tuff ring and maar morphologies, which contain a series of volcanic units up to 100 m thick (Campeny et al., 2014). The eruptive activity in the area was predominantly explosive, since most of the volcanic series are pyroclastics. However, effusive activity is also reported (Campeny et al., 2014), and four outcrops of carbonatite lavas - Huilala-Ungongué, Ipunda, Jango and Utihohala, have been described (Fig. 1).

The Catanda carbonatites are structurally associated with the Lucapa corridor, an extensional belt oriented NE-SW across the Congo-Kassai craton, related to the break-up of Gondwana during the Cretaceous (Issa Filho et al., 1991). Most of the Angolan carbonatites are distributed along this rift including Virulundo, Tchivira-Bonga, Bailundo or Longonjo (Torró et al., 2012; Melgarejo et al., 2012; Calvo et al., 2011a, b), along with kimberlites including the Catoca pipe (Robles-Cruz

et al., 2012; Korolev et al., 2014), which is one of the most productive diamond mines in the African continent.

The volcanic activity in the Catanda region has never been precisely dated. Silva and Pereira (1973) proposed a 92 Ma (± 7) K-Ar age (Torquato and Amaral, 1973) for a tinguaitite dyke assumed to be contemporaneous with the carbonatite outcrops. This age is younger than the formation of the Lucapa corridor and the Catoca kimberlite, dated as Early Cretaceous (Robles-Cruz et al., 2012). However, the occurrence of multiple episodes of magmatic activity, including those during the Cretaceous, cannot be ruled out and future accurate dating is highly desirable in the area.

3. Analytical methods

Textural and mineralogical studies were carried out by optical microscopy as well as with an E-SEM-Quanta 200 FEI-XTE-325/D8395.BSE Scanning Electron Microscope with a Genesis EDS micro-analysis system, at the Scientific and Technical Centre of the University of Barcelona (CCiTUB). Operating conditions were 25 kV, 1 nA beam current and 15 mm distance to detector.

Whole rock major and trace element analyses were performed by conventional X-ray fluorescence (XRF) and ICP-emission spectrometry following a lithium metaborate/tetraborate fusion and nitric acid digestion at the ACME Analytical Laboratories Ltd. from Vancouver, Canada.

Calcite, magnetite, fluorapatite, and phlogopite compositions were analysed with wavelength-dispersive spectrometry (EPMA-WDS) at CCiTUB, using a Cameca SX50 electron microprobe. Results were processed using the PAP matrix correction programme (Pichou and Pichoir, 1984). Operating conditions were an accelerating voltage of 15–20 kV combined with a beam current of 5 to 20 nA and a 10–15 μm spot beam diameter. Standards used for the analyses were: fluorite (F, K α); albite (Na, K α); periclase (Mg, K α); Al₂O₃ (Al, K α); diopside (Si, K α); fluorapatite (P, K α); AgCl₂ (Cl, K α); orthoclase (K, K α);

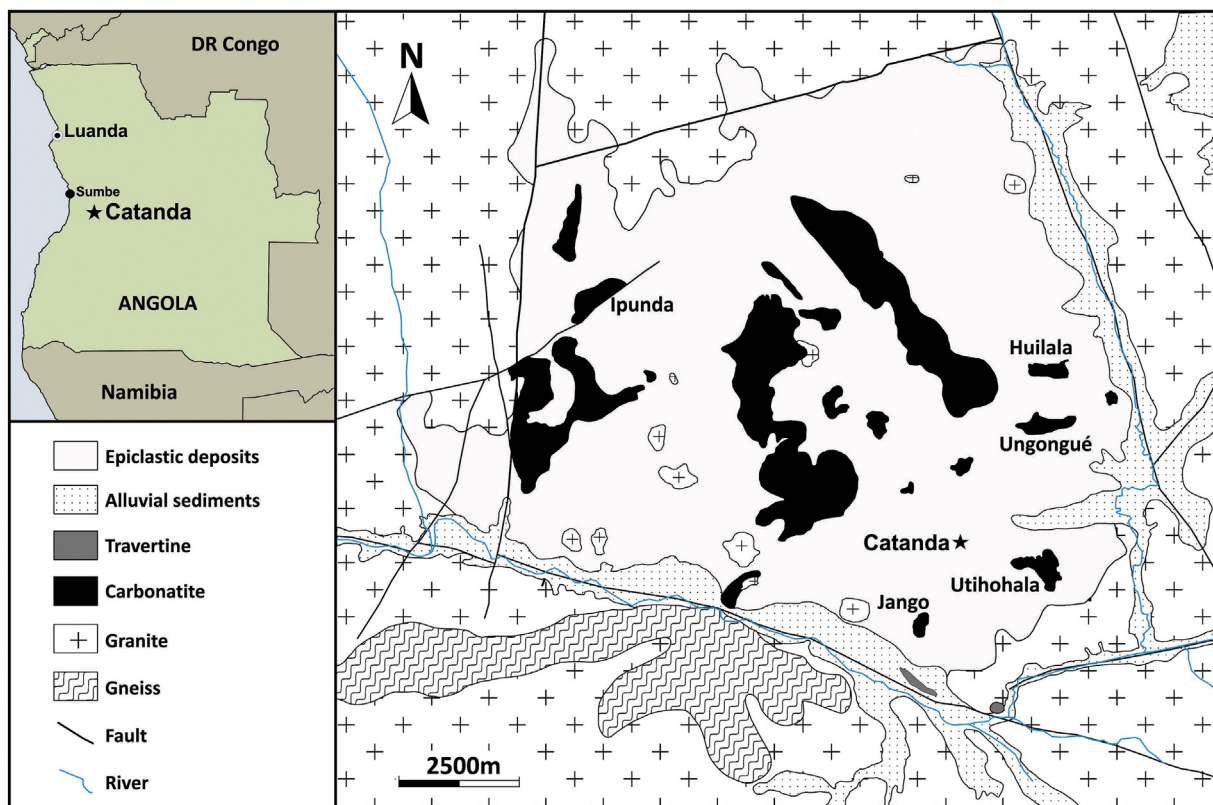


Fig. 1. Geographic location and geological map of the Catanda area.

wollastonite (Ca, $\text{K}\alpha$); rutile (Ti, $\text{K}\alpha$); metallic vanadium (V, $\text{K}\alpha$); Cr_2O_3 (Cr, $\text{K}\alpha$); rhodonite (Mn, $\text{K}\alpha$); Fe_2O_3 (Fe, $\text{K}\alpha$); sphalerite (Zn, $\text{K}\alpha$); celestine (Sr, $\text{L}\alpha$); LaB_6 (La, $\text{L}\alpha$) and CeO_2 (Ce, $\text{L}\alpha$).

Trace element compositions of calcite were analysed using Coherent COMPex Pro-ArF Excimer LA-ICP-MS equipment at the School of Earth Sciences of the University of Tasmania (Australia). This instrumentation consists of a New Wave Research UP213 Nd-YAG (213 nm) laser coupled to an Agilent 7500 quadrupole mass spectrometer. Analyses were performed in a He atmosphere by ablating 35–100 μm spots, at a rate of 10 shots using a laser power of $\sim 3.2 \text{ J/cm}^2$. The analysis time for each sample was 70 s, and comprised a 25 second background measurement (laser off) and a 45 second analysis with laser on. Instrument calibration was carried out ablating the NIST612 glass standard. Data reduction was undertaken by standard methods (Longerich et al., 1996) using the NIST612 glass as a primary reference material (values from Pearce et al., 1997). USGS BCR-2g glass was repeatedly analysed throughout the analytical sessions and was used as a secondary standard.

Stable isotope analyses of C and O were carried out in the Isotope-ratio mass spectrometry (IRMS) laboratory of the CCITUB. The CO_2 extraction was carried out in a Thermo Finnigan Kiel Carbonate Device III, which reproduces an automated modified version of the McCrea method (McCrea, 1950). Powdered carbonate samples (50–60 μg) are digested by H_3PO_4 at 70°C for 3 minutes. The generated CO_2 is analysed by an isotope ratio mass spectrometer Thermo Finnigan MAT-252, which is coupled to the Carbonate Device. Analytical calculations are processed by software Isodat 2.0 and results are calibrated using IAEA international reference materials NBS-18 ($\delta^{13}\text{C}$ (PDB) = -5.1% ; $\delta^{18}\text{O}$ (V-SMOW) = -23.2%) and NBS-19 ($\delta^{13}\text{C}$ (PDB) = $+1.95\%$; $\delta^{18}\text{O}$ (PDB) = -2.20%) digested during 7 minutes. The standard deviation of measurements was 0.06 for $\delta^{13}\text{C}$ and 0.05 for $\delta^{18}\text{O}$.

Melt inclusion studies were performed using petrographic microscopy, scanning electron microscopy using a FEI Quanta 600 MLA ESEM coupled with energy dispersive X-ray spectroscopy analysis, and a Hitachi SU-70 Field Emission Scanning Electron Microscope (FESEM) at the Central Science Laboratory of the University of Tasmania (Australia).

4. Petrography

Four outcrops of carbonatite lavas are identified in the Catanda area (Campeny et al., 2014), namely Huilala-Ungongué, Ipunda, Jango and Utihohala, distinct in their mineralogical and textural characteristics (Table 1).

4.1. Huilala-Ungongué

These carbonatite lavas are located in the Huilala and the Ungongué hills (Fig. 1) in outcrops formed by an alternating series of lavas and lapilli tuffs (Campeny et al., 2014). Huilala-Ungongué lavas are fine-grained porphyritic dark grey rocks with a very low modal percentage of carbonates (≈ 30 modal %). Microphenocrysts comprise up to ≈ 20 modal %, and they are mainly fluorapatite (35 modal %), magnetite (35 modal %), titaniferous augite (15 modal %) and phlogopite (15 modal %). Fluorapatite microphenocrysts form subhedral grains consisting of hexagonal prisms and pinacoids with a short prismatic habit up to 1 mm across, which are occasionally strongly zoned. Magnetite is present as euhedral crystals up to 0.5–1 mm in diameter (Fig. 2a), occasionally fractured and presenting corroded borders. They also exhibit a marked concentric zoning, forming typical atoll textures and contain inclusions of minerals such as perovskite, pyrite and pyrrhotite. Titaniferous augite is present as subhedral rounded microphenocrysts of 1 to 2 mm that may replace magnetite (Fig. 2a); some augite crystals show a marked compositional zoning. Phlogopite grains form zoned angular crystals up to 3 mm across.

The rock is up to 80 modal % groundmass, which has a very complex mineral assemblage (Fig. 2b). Fine grained calcite is dominant and is accompanied by accessory minerals such as fluorapatite, magnetite, cuspidine, perovskite, pyrochlore, baddeleyite, periclase, brucite and scarce grains of zirconolite, spurrite and very rare oldhamite. Groundmass fluorapatite is present as zoned euhedral crystals up to 100 μm in length, while magnetite generally forms zoned euhedral grains up to 200 μm . Cuspidine, which is commonly intergrown with fluorapatite grains, forms short euhedral to subhedral prismatic crystals up to 50 μm (Fig. 2c). Perovskite is present as euhedral to subhedral grains up to 40 μm in size, with very marked compositional zoning (Fig. 2d). Pyrochlore is another common mineral in the groundmass. It is typically included in calcite, but it may also occur as inclusions in other minerals such as magnetite or brucite (Fig. 2e). Pyrochlore occurs as small euhedral grains, less than 20 μm in diameter, often slightly corroded. It is generally well zoned and up to three generations of pyrochlore may be distinguished in some grains (Bambi et al., 2012; Melgarejo et al., 2012). Brucite is widely present in the Huilala-Ungongué samples, typically as pseudomorphs after primary grains of periclase. This replacement is typically completed, but subhedral periclase crystals of 5 to 10 μm may still be preserved as cores with altered rims of brucite (Fig. 2f). Periclase grains contain inclusions of magnetite, perovskite, fine-grained pyrochlore and baddeleyite, occurring as 5 to 10 μm anhedral grains. These minerals are also commonly included in other minerals such as

Table 1
Mineralogical and textural comparison of the different carbonatite lava locations reported in the Catanda area.

Location	Texture	Carbonate content (modal %)	Mineralogy
Huilala - Ungongué	Finely porphyritic	~ 30	Microphenocrysts: fluorapatite (35%), titaniferous magnetite (35%), augite (15%), phlogopite (15%) Groundmass: calcite, fluorapatite, titaniferous magnetite, pyrochlore, baddeleyite, cuspidine, perovskite, periclase, brucite, zirconolite, spurrite, oldhamite Xenocrysts: olivine, quartz, microcline Secondary: sparry calcite, barite, rhabdophane, crandallite
Ipunda	Trachytoid	~ 70	Microphenocrysts: calcite (60%), fluorapatite (15%), titaniferous magnetite (15%), phlogopite (5%), augite (5%) Groundmass: calcite, fluorapatite, titaniferous magnetite, pyrochlore, baddeleyite Xenocrysts: quartz, microcline Secondary: sparry calcite
Jango	Finely porphyritic	~ 70	Phenocrysts: fluorapatite (60%), titaniferous magnetite (25%), phlogopite (10%), augite (5%) Groundmass: calcite, fluorapatite, titaniferous magnetite, pyrochlore, baddeleyite, monticellite Xenocrysts: amphibole, quartz, microcline Secondary: sparry calcite
Utihohala	Finely porphyritic	~ 60	Microphenocrysts: fluorapatite (60%), titaniferous magnetite (20%), phlogopite (15%), augite (5%) Groundmass: calcite, fluorapatite, titaniferous magnetite, pyrochlore, alabandite Xenocrysts: quartz, microcline Secondary: sparry calcite

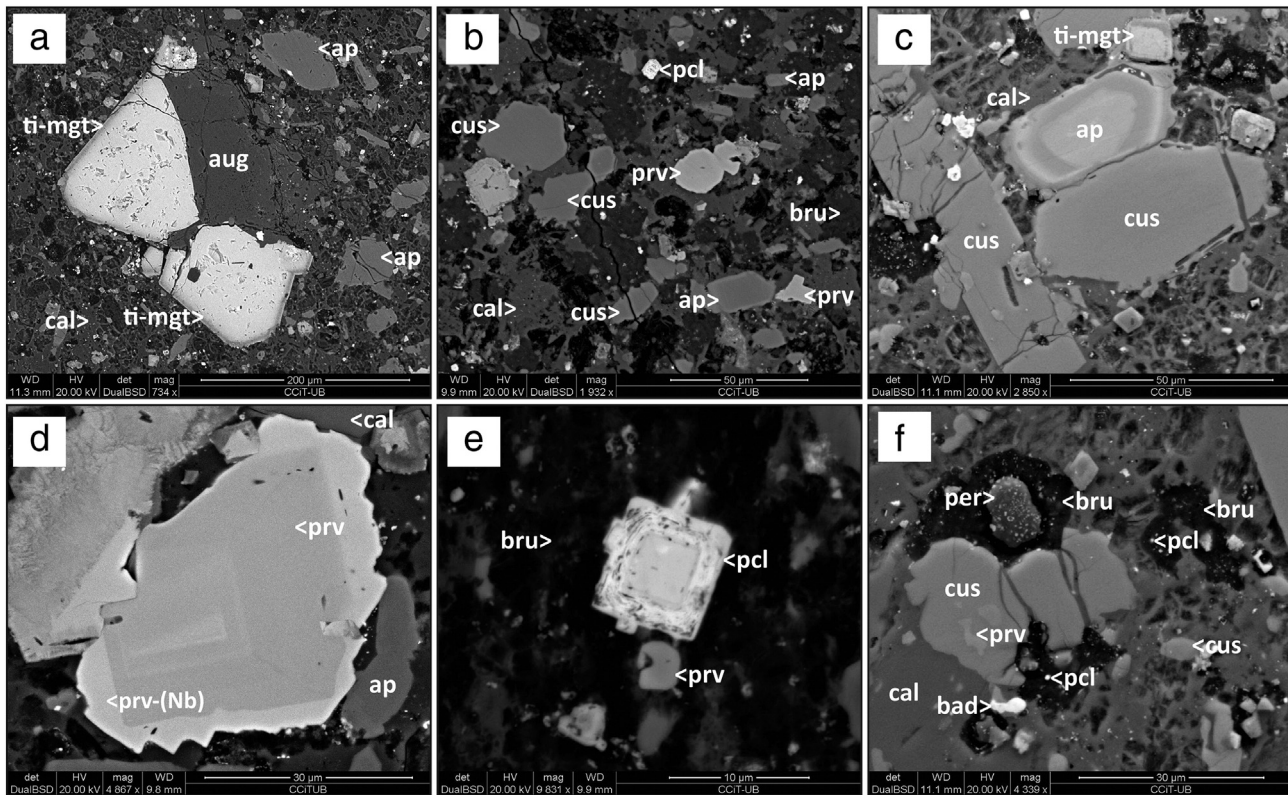


Fig. 2. SEM (BSE) images of the Huilala-Ungongué lavas. **a** Microphenocrysts of fluorapatite (ap) and titaniferous magnetite (ti-mgt) partially replaced by augite (aug) which also infill small fractures. **b** Typical mineral association of the Huilala-Ungongué groundmass: fluorapatite (ap), cuspidine (cus), pyrochlore (pcl), perovskite (prv), fine grained calcite (cal) and secondary brucite (bru). **c** Basal section of zoned fluorapatite (ap) associated with euhedral grains of cuspidine (cus) and titaniferous magnetite (ti-mgt). **d** Euhedral crystal of perovskite showing extreme compositional zoning with rims enriched in Nb. **e** Euhedral grains of zoned pyrochlore (pcl) and perovskite (prv) inside a typical halo of brucite (bru). **f** Preserved grain of periclase (per) surrounded by secondary brucite (bru) associated with cuspidine (cus) with perovskite (prv) and baddeleyite inclusions. Small grains of pyrochlore are also present inside the brucite halos.

perovskite and magnetite. Spurrite is a very scarce phase sometimes associated with cuspidine as anhedral grains of less than 5–10 μm . Rare zirconolite and oldhamite crystals of less than 10 μm in diameter are occasionally found as inclusions in other minerals.

Subhedral grains of barite up to 0.5 mm are also common as well as occasional secondary fibrous thaumasite and phosphates such as rhabdophane or crandallite.

4.2. Ipunda

Ipunda lavas are cream-colored fine-grained porphyritic rocks, with ≈ 70 modal % calcite. They are characterised by a very distinctive trachtyoid texture made up of tabular calcite microphenocrysts dominating an interstitial sparry carbonate matrix (Fig. 3a). The microphenocrysts are colourless tabular grains (60 modal %) up to 1 mm in length, accompanied by strongly zoned magnetite (15 modal %) up to 1 mm and euhedral grains of fluorapatite (15 modal %) up to 2 mm in length, with concentric zoning and abundant fluid inclusions trapped at the crystal cores. Phlogopite (5 modal %) crystals up to 1 mm and very scarce grains of zoned augite (5 modal %) are also present as microphenocrysts.

The mineralogy of the groundmass is very simple compared to the Huilala-Ungongué lavas. Fine-grained calcite is the dominant phase (75 modal %); fluorapatite (10 modal %) (Figs. 3b and c) and magnetite (5 modal %) are also present. The rest of accessory minerals account for only approximately 5 modal % and are euhedral zoned grains of pyrochlore, less than 20 μm in diameter and scarce anhedral baddeleyite grains of less than 10 μm , mostly included in magnetite crystals.

Spherical globules up to 1 mm in diameter are abundant in the matrix and are completely infilled by secondary sparry calcite with minor goethite inclusions (Figs. 3b and c).

4.3. Utihohala

Utihohala rocks are fine-grained porphyritic (Fig. 4a) dark brown lavas containing ≈ 60 modal % carbonates. Microphenocrysts represent around 25 modal % and are prismatic grains of apatite up to 2 mm (50 modal %), as well as strongly zoned magnetite grains up to 2 mm in size (30 modal %). Prismatic euhedral phlogopite (15 modal %) up to 1 mm across and zoned augite (5 modal %) grains up to 0.5 mm are also present (Fig. 4a).

The groundmass occupies 75 modal % and it is mainly calcite (60 modal %), fluorapatite (10 modal %) (Fig. 4b), magnetite (10 modal %) and a small proportion of accessory minerals (≈ 10 modal %) such as euhedral grains of pyrochlore up to 20 μm , scarce grains of baddeleyite up to 15 μm and euhedral crystals of alabandite up to 5 μm , which, in Catanda, were only found in these lavas.

4.4. Jango

The mineralogy and textures of the Jango lavas are very similar to those in the Utihohala area. The Jango lavas are brown fine-grained porphyritic textured rocks (Fig. 4c) with ≈ 70 modal % carbonates, significantly higher than the Huilala-Ungongué lavas.

Microphenocrysts are sparse (≈ 20 modal %) in an abundant groundmass. They are principally euhedral grains of fluorapatite up to 1 mm in diameter (60 modal %), euhedral zoned crystals of magnetite

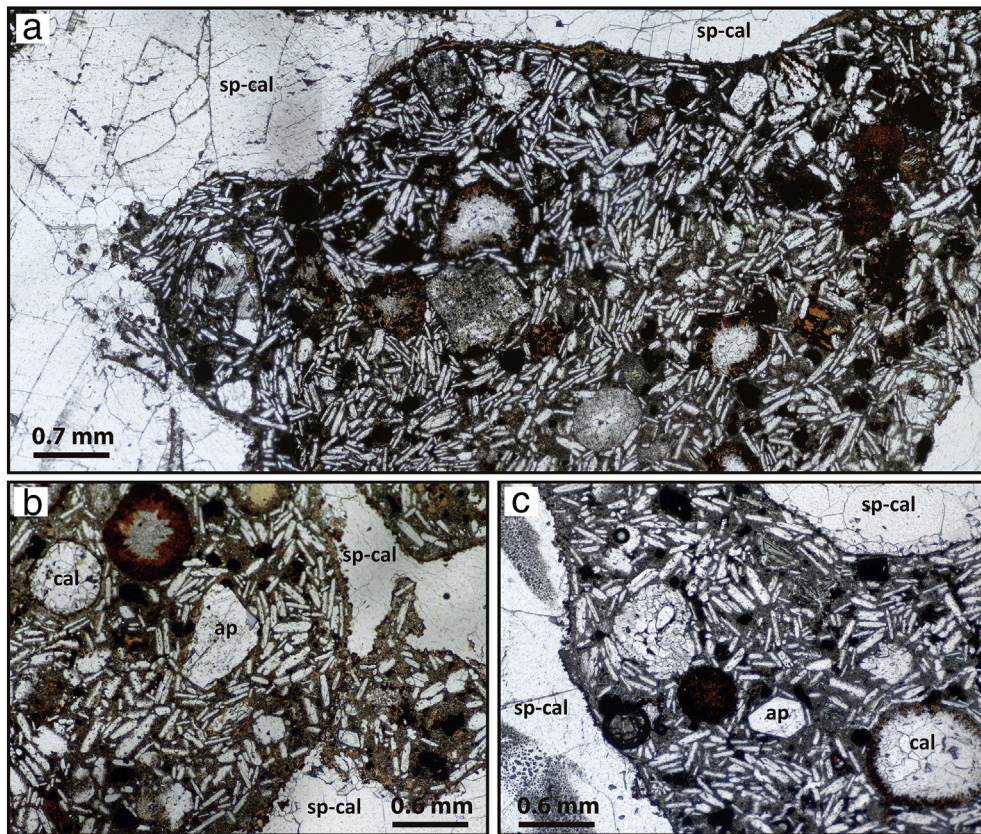


Fig. 3. Plane-polarized light photomicrographs of Ipunda lavas. **a** General view of a Ipunda lava sample distinguished by its distinctive trachtyoid texture of tabular calcite phenocrysts. Secondary sparry calcite (sp-cal) is also present. **b** Ipunda lava with fluorapatite (ap) phenocrysts and spherical globules filled by calcite (cal). **c** Euhedral phenocryst of apatite (ap) accompanied by tabular calcite and typical spherical globules filled with calcite (cal) and secondary iron oxides.

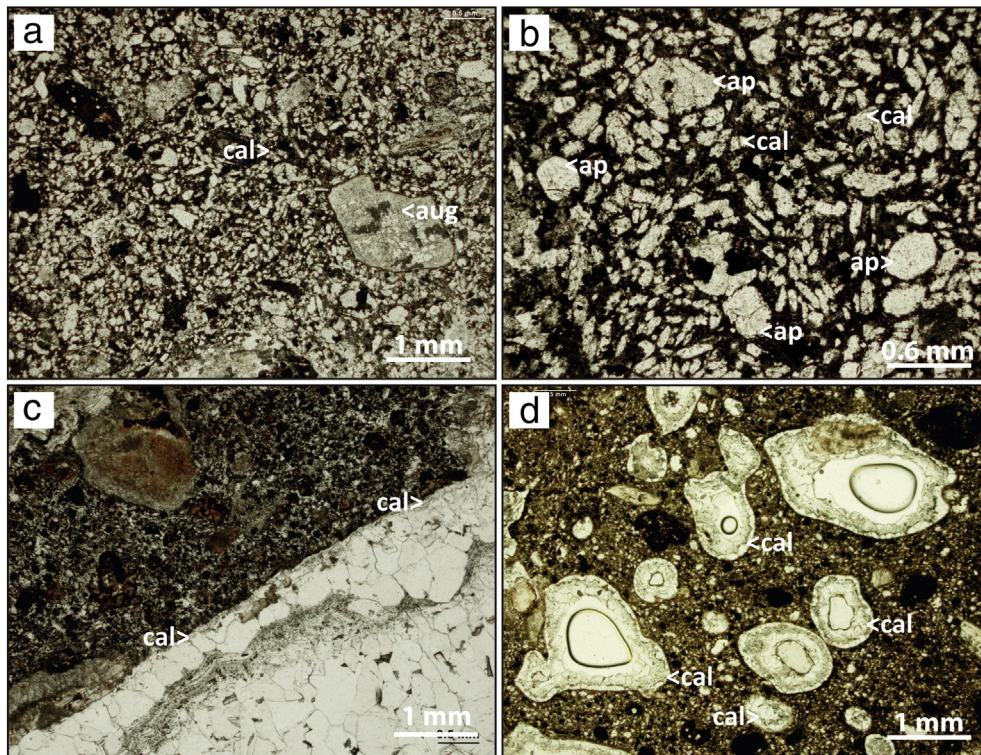


Fig. 4. Plane-polarized light photomicrographs of the Utihohala and Jango lavas **a** General view of a Utihohala sample. Augite (aug) microphenocrysts in calcitic (cal) groundmass. **b** Subhedral grains of fluorapatite (ap) and calcite (cal) in the Utihohala lava groundmass. **c** General view of the Jango lava sample with secondary calcite (cal) infilling a fracture. **d** Jango lava sample with typical cavities partially infilled by secondary calcite (cal).

up to 2 mm (25 modal %) in which is also possible to distinguish atoll textures, as well as euhedral grains of phlogopite (10 modal %) up to 2 mm and scarce zoned augite (5 modal %) up to 0.5 mm.

The groundmass, (≈ 80 modal %) is mainly fine-grained calcite (65 modal %), fluorapatite (15 modal %), magnetite (10 modal %) and accessory minerals (10 modal %) such as zoned euhedral crystals of pyrochlore up to 10 μm , subhedral prismatic monticellite crystals up to 30 μm , and scarce subhedral grains of baddeleyite up to 15 μm mostly as inclusions in magnetite.

Fractures filled by sparry calcite are common (Fig. 4c) as well as vesicles up to 3 mm partially filled by sparry carbonates (Fig. 4d).

4.5. Xenoliths

In all lava types xenocrystic material is less than about 5 modal %. The most common xenoliths in the Catanda lavas are, by far, highly fenitized granitic rocks derived from the underlying Archaean granites. They form fragments up to 4 cm; individual grains of quartz, microcline and plagioclase are also common as xenocrysts. Rounded xenoliths of glimmerite and amphibolite are occasionally present in the Catanda lavas. In the Huilala-Ungongué lavas there are occasional rounded grains of olivine (Peres et al., 1968) up to 5 mm in diameter, usually replaced by serpentine and fine-grained iron oxides.

5. Mineral chemistry

The four major microphenocryst mineral phases in all Catanda lavas: calcite, spinel, fluorapatite and phlogopite, were selected to study their chemical composition.

5.1. Calcite

Calcite is the dominant magmatic carbonate in all the Catanda lavas; other carbonates such as dolomite, ankerite or siderite are not present either as microphenocrysts or in the groundmass. The major element

composition of calcite is homogeneous in all carbonatite lavas, but trace elements present significant differences (Supplementary Table A.1). These trace element differences are also reflected in the response of Catanda carbonates to cold cathodoluminescence, since cathodoluminescence is related to factors including the presence of some trace elements acting as activators such as Mn^{2+} and REEs (Habermann et al., 1996). In general, Catanda calcite emits a strong orange glow, but this glow is completely absent in the typical sparry grains present in all lava types. It is also remarkable that, under cold cathodoluminescence, tabular calcite microphenocrysts of the Ipunda lavas, which form a typical trachytoid texture, exhibit a marked concentric zoning (Figs. 5a and b).

5.2. Spinel

Spinel group minerals from Catanda have very heterogeneous compositions due to extreme zoning present in most grains. However, in general, they correspond to magnetite with high Ti concentration, up to 14.4 wt.% TiO_2 (0.130 to 0.408 apfu of Ti, Supplementary Table A.2). Aluminium contents are also high, up to 14.3 wt.% Al_2O_3 , higher than those reported in other carbonatite localities such as the Kerimasi volcano (Reguir et al., 2008; Guzmics et al., 2015), but similar to the spinels analysed in the Fort Portal volcanic carbonatites, which present the highest Al contents reported in magnetite from carbonatites (Bailey and Kearns, 2002; Reguir et al., 2008). The spinel from Catanda are also moderately enriched in Mg, with contents ranging from 4.9 to 12.0 wt.% MgO, similar to those described in other volcanic carbonatite localities such as Kerimasi (Tanzania) (Reguir et al., 2008; Guzmics et al., 2015) or Fort Portal (Uganda) (Bailey and Kearns, 2002). The relation between #Ti [Ti/(Ti+Cr+Al)] and #Fe [Fe/(Fe+Mg)] shows a clear titanomagnetite trend (Fig. 6) such as typically described in some kimberlites (Boctor and Boyd, 1982; Rozova et al., 1982) and aillikite localities (Tappe et al., 2006). Another significant compositional feature of the analysed spinels is the low content of Cr, which is always below 0.1 wt.% Cr_2O_3 (Supplementary Table A.2).

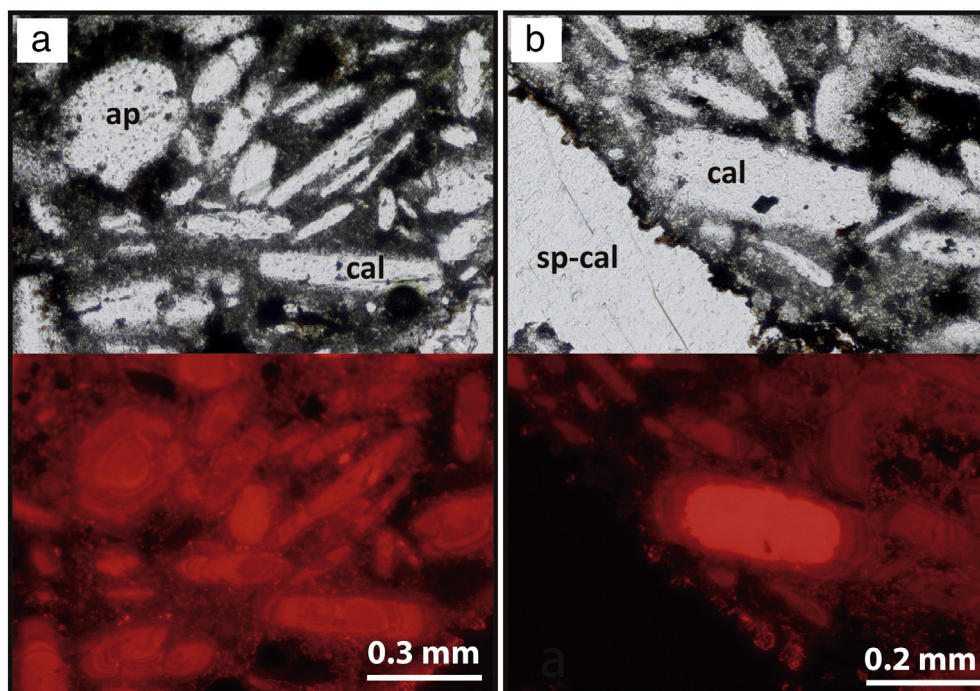


Fig. 5. **a** Ipunda sample. Euhedral fluorapatite (ap) section and tabular crystals of calcite (cal). Cathodoluminescence response of calcite is distinguished by a marked orange glow and fluorapatite exhibits concentric zoning. **b** Tabular phenocrysts of calcite (cal) show a marked zoning under cold cathodoluminescence while secondary sparry calcite (sp-cal) does not exhibit any response at all.

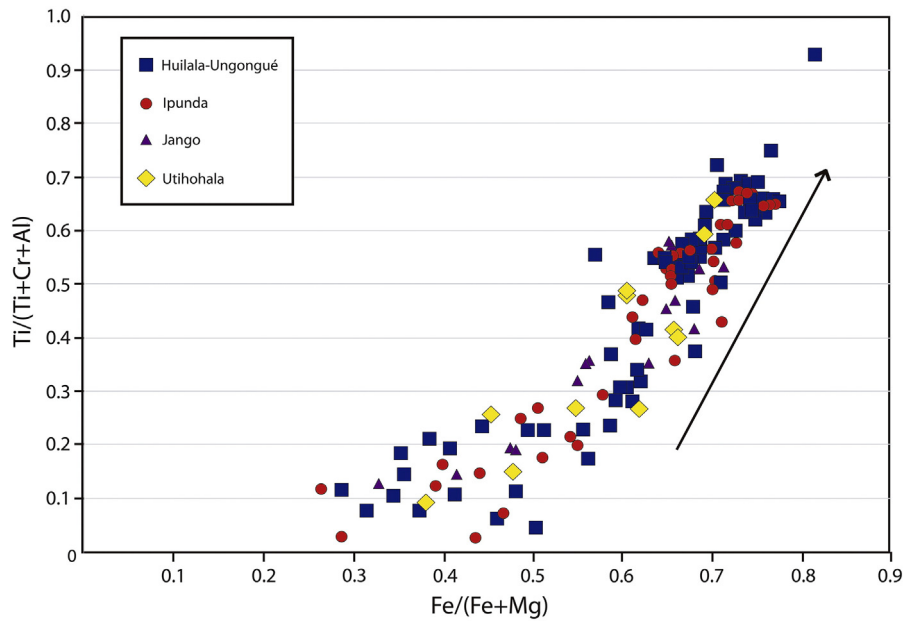


Fig. 6. Relation between $\text{Fe}/(\text{Fe}+\text{Mg})$ and $\text{Ti}/(\text{Ti}+\text{Cr}+\text{Al})$ in the Catanda magnetite showing a typical "titanomagnetite trend" according to Mitchell (1986).

5.3. Fluorapatite

Fluorapatite is present as microphenocrysts as well as in the ground-mass in all of the Catanda lavas, and its composition does not present significant differences among the four lava locations. In general, fluorapatite has low concentrations of Mn and Na, while it is slightly enriched in Sr, ranging from 0.3 to 1.4 wt.% (Supplementary Table A.3). Catanda fluorapatite is especially rich in *Light Rare Earth Elements* (LREE) with La contents between 670 and 990 ppm and Ce ranging from 1700 to 2460 ppm (Supplementary Table A.3). This enrichment is generally marked by a strong compositional zoning due to the concentration of REE in the grain rims, which are also enriched in SiO_2 .

5.4. Phlogopite

Phlogopite occurs as microphenocrysts in all the Catanda lavas and has similar compositions in all of them. In general, Catanda phlogopite is enriched in TiO_2 , ranging from 1.17 to 4.2 wt.% (Supplementary Table A.4) and also has significant contents of Ba, especially in the Huilala-Ungongué samples with contents up to 0.39 wt.% BaO (Supplementary Table A.4).

6. Geochemistry

The outcropping lavas of the Huilala-Ungongué area (Fig. 1) are the most enriched in SiO_2 , with contents varying between 14.3 and 23.3 wt.% (Supplementary Table A.5). Similar silica contents in carbonatites have been reported in the lavas from Fort Portal (Uganda) (Eby et al., 2009), as well as in other carbonate-rich rocks such as the aillikites from Aillik Bay in (Canada) and Tikiusaaq (Greenland) (Tappe et al., 2006; 2009). However, the lavas from Ipunda, Jango and Utihohala (Fig. 1) have lower SiO_2 concentrations, ranging from 6.3 to 12.7 wt.%. In general, the Huilala-Ungongué lavas are also enriched in Ti, Al and Fe compared to the other localities, which are also distinguished by a relative enrichment in CaO, with values up to 46.5 wt.% (Supplementary Table A.5).

All the lava types from the Catanda area are impoverished in alkalis, with K and Na contents well below 1 wt.%.

Fluorine is variable depending on the lava outcrop. The highest concentrations are found in the Huilala-Ungongué and Utihohala lavas with

values from 4470 to 6790 and 6850 ppm respectively, while in the rest fluorine is lower, varying from 4040 to 4330 ppm in Jango and only 1570 ppm in the Ipunda outcrops (Supplementary Table A.5).

In general, the Catanda carbonatite lavas are distinguished by REE contents between 1100 and 3000 ppm, higher than those described in other extrusive carbonatite localities such as Fort Portal (Eby et al., 2009). HFSE contents are generally high in all types of lavas. Niobium is the most abundant HFSE with values between 281 to 706 ppm, while Ta values reach 23 ppm, which are relatively high compared to average of other carbonatite localities (Chakhmouradian, 2006). The Nb/Ta ratio of Catanda lavas are between 21 and 37 which are typical values of carbonatites (Chakhmouradian, 2006).

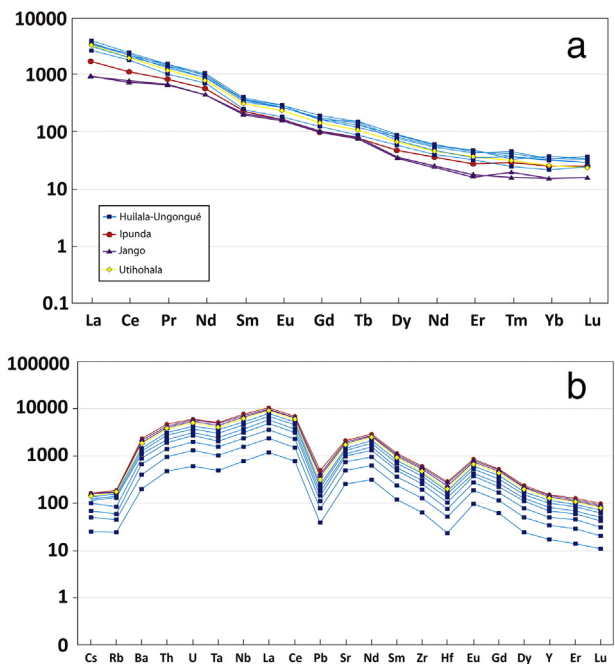


Fig. 7. **a** REE plot of Catanda carbonatite lavas normalized to chondrite. **b** Multi-elemental trace element composition of Catanda carbonatite lavas normalized to primitive mantle. Normalization values in both diagrams from Sun and McDonough (1989).

REE diagrams of carbonatite lavas from Catanda do not show clear differences between the different lavas. All patterns present a marked negative slope showing a strong enrichment in light REE relative to heavy REE (Fig. 7a).

As in the REE diagrams, multi-elemental diagrams show very similar patterns between the four lava locations (Fig. 7b).

7. Stable isotopes

Supplementary Table A.6 presents the stable isotope composition ($\delta^{13}\text{C}$ and $\delta^{18}\text{O}$) of the Catanda groundmass carbonates. Two samples of secondary sparry carbonate infilling cavities of the lavas, as well as a sample from the Pedra de Água travertine deposit were added to compare carbonatite data with these secondary and surficial carbonates (Fig. 1).

The $\delta^{18}\text{O}_{(\text{V-SMOW})}$ compositions are very heterogeneous, with values ranging from 9.4 to 17.9 ‰ $\delta^{18}\text{O}$ (Supplementary Table A.6). On the other hand, secondary sparry carbonate and the travertine samples show much higher oxygen isotope composition compared to magmatic carbonates with $\delta^{18}\text{O}_{(\text{V-SMOW})}$ values between 26.4 and 27.2 ‰ $\delta^{18}\text{O}$.

Carbon isotope compositions are similar in the Ipunda, Jango and Utihohala magmatic carbonates with values ranging from -5.2 to -5.6 ‰ $\delta^{13}\text{C}_{(\text{V-PDB})}$. On the other hand, Huilala-Ungongué lavas show marked differences to the other localities, presenting lower $\delta^{13}\text{C}$ compositions with values from -8.1 to -12.2 ‰ $\delta^{13}\text{C}$. Secondary carbonate $\delta^{13}\text{C}$ values are significantly higher and more variable than in the lavas ($\delta^{13}\text{C}$ values between -4.2 and -1.0 ‰), while the Pedra de Água travertine present $\delta^{13}\text{C}$ of 6.4 ‰, which is the highest carbon isotope composition reported in the rocks from the Catanda area.

8. Melt inclusions

The mineralogical study of the Catanda lavas were complemented with the analysis of the melt inclusions assemblages preserved in magnetite grains. Approximately 200 melt inclusions, with sizes varying from 5 to 25 μm , were studied from all carbonatite lava localities

Table 2

List of the mineral phases identified in the melt inclusion assemblage hosted by magnetite phenocrysts of the Catanda lavas.

	Mineral	Ideal Formula	Occurrence distribution (%)
Carbonates	Calcite	CaCO_3	59.5
	Dolomite	$\text{CaMg}(\text{CO}_3)_2$	6
	Northupite	$\text{Na}_3\text{Mg}(\text{CO}_3)_2\text{Cl}$	1.2
	Nyerereite	$\text{Na}_2\text{Ca}(\text{CO}_3)_2$	50
	Shortite	$\text{Na}_2\text{Ca}_2(\text{CO}_3)_3$	
	Trona	$\text{Na}_3\text{H}(\text{CO}_3)_2 \cdot 2 \text{H}_2\text{O}$	6
Halides	Halite	NaCl	8.3
	Neighborite	NaMgF_3	2.4
	Sylvite	KCl	4.8
Silicates	Cuspidine	$\text{Ca}_4(\text{Si}_2\text{O}_7)(\text{F},\text{OH})_2$	8.3
	Diopside	$\text{CaMgSi}_2\text{O}_6$	19
	Forsterite	Mg_2SiO_4	7.1
	Humite	$(\text{Mg},\text{Fe}^{2+})_7(\text{SiO}_4)_3(\text{F},\text{OH})_2$	1.2
	Nepheline	$(\text{Na},\text{K})\text{AlSiO}_4$	26.2
	Phlogopite	$\text{KMg}_3(\text{AlSi}_3\text{O}_{10})(\text{OH},\text{F})_2$	9.5
	Sodalite	$\text{Na}_8(\text{Al}_6\text{Si}_6\text{O}_{24})(\text{Cl},\text{S})_2$	3.6
Sulphides	Pyrite	FeS_2	23.8
	Pyrrhotite	Fe_{1-x}S	7.1
	Rasvumite	KFe_2S_3	6
Oxides	Magnetite	$\text{Fe}^{2+}\text{Fe}^{3+}_2\text{O}_4$	10.7
	Periclase	MgO	1.2
	Perovskite	CaTiO_3	41.7
	Pyrochlore	$(\text{Na},\text{Ca},\text{Pb},\text{U})_2\text{Nb}_2(\text{O},\text{OH})_6(\text{OH},\text{F},\text{O})$	4.8
Phosphates	Fluorapatite	$\text{Ca}_5(\text{PO}_4)_3\text{F}$	47.6

reported in the Catanda area, and 24 daughter phases have been identified. These minerals, including calcite, fluorapatite, perovskite and cuspidine, are generally present in the lavas, although other phases are exclusive to the melt inclusions assemblage, and have been not described as microphenocrysts or in the lavas groundmass (Table 2). In addition, despite the generally low alkali contents of the Catanda lavas, up to 12 of the 24 daughter phases described in the melt inclusions are alkali-rich, e.g. carbonates such as trona (Fig. 8a) shortite (Figs. 8b and d) and nyerereite, halides such as halite and sylvite (Fig. 8c) and silicates such as sodalite and nepheline (Fig. 8b).

9. Discussion

9.1. Classification of the Catanda lavas

In the Catanda area, two main types of carbonatitic lavas may be defined based on their carbonate contents and chemical composition: calciocarbonatites and silicocarbonatites.

Calciocarbonatites occur in the Ipunda, Jango and Utihohala areas. Their modal carbonate contents are higher than 50%, corresponding to normal carbonatites according to the classification of Le Maitre (2002). However, strong textural differences may be established between these three localities. Jango and Utihohala lavas present finely porphyritic textures formed by fluorapatite, magnetite, phlogopite and minor augite microphenocrysts hosted in a calcite rich groundmass (Table 1), while Ipunda lava is characterised by a trachytoid texture formed by tabular microphenocrysts of calcite.

The Ipunda texture is similar to that described in other carbonatite localities such as the Koru Beds from Tinderet (Kenya), the carbonatites from Homa Mountain (Kenya), the spherical lapilli of the Rockeskyll complex (Germany) or the carbonatite tephros of the Kerimasi volcano (Tanzania) (Deans and Roberts, 1984; Clark and Roberts, 1986; Keller, 1981; Riley et al., 1996; Hay, 1983). In the Kerimasi tephra, calcite also shows concentric zoning under cold cathodoluminescence (Mariano and Roedder, 1983) as also described in the Ipunda lavas (Fig. 5). The origin of these trachytoid textures has been controversial over time, until Zaitsev et al. (2013) studied them in Tinderet and concluded that calcite tabular crystals were formed by alteration of primary alkaline carbonates. It is well known that alkaline carbonates such as nyerereite or gregoryite are very unstable, and easily altered to calcium carbonates during secondary weathering processes, as described in the Oldoinyo Lengai natrocarbonatite flows (Zaitsev and Keller, 2006). In our view, Ipunda trachytoid texture is also due to the alteration of primary alkaline carbonates; subsequently pseudomorphed to calcite in an analogous process as proposed for Tinderet (Zaitsev et al., 2013) and also probably occurred in other carbonatite localities with similar textures.

On the other hand, silicocarbonatites from the Catanda area are present in the Huilala-Ungongué outcrops. These lavas are significantly enriched in SiO_2 (Supplementary Table A.4) and present a finely porphyritic texture in which microphenocrysts are made up of fluorapatite, phlogopite, augite and magnetite, hosted in a calcite rich groundmass which also contain other accessory phases such as cuspidine, pyrochlore, perovskite and periclase. Similar SiO_2 contents and mineralogy have been reported in other silica-rich carbonatite lavas such as in Fort Portal (Uganda) or in the aillikites from Aillik Bay (Canada) (Eby et al., 2009; Tappe et al., 2006).

Hence, the four carbonatitic lavas described in Catanda, which present several compositional, textural and mineralogical differences may be classified as calciocarbonatites (Jango and Utihohala), secondary calciocarbonatites produced by the alteration of primary natrocarbonatite lavas (Ipunda) and silicocarbonatites (Huilala-Ungongué).

9.2. Parental magma composition

Trace element contents are similar for all lava locations and the REE and multi-elemental diagrams (Fig. 7) also present very similar patterns

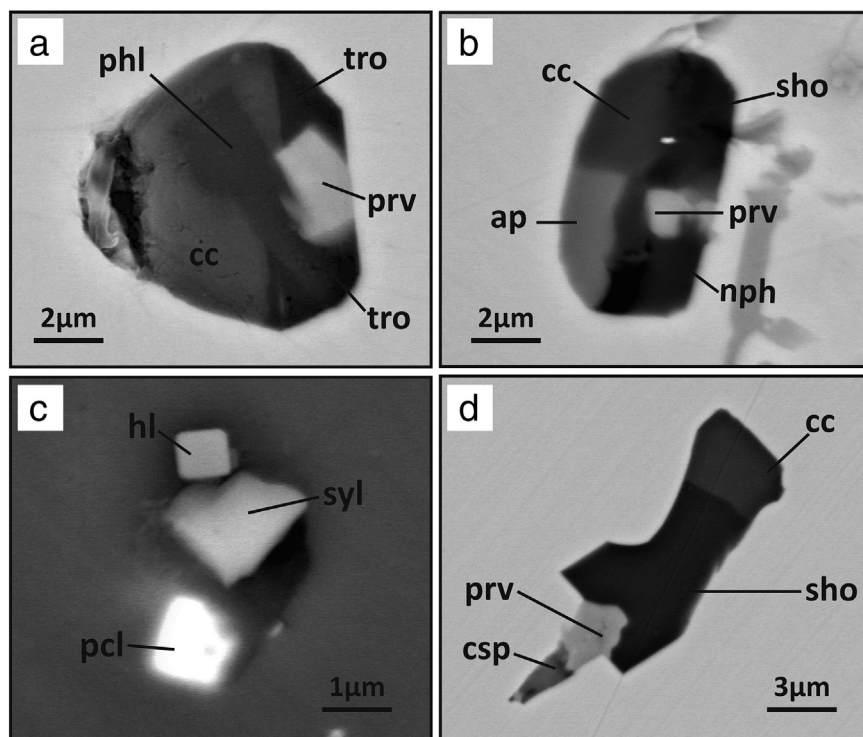


Fig. 8. SEM (BSE) images of melt inclusions in magnetite of Catanda lavas. **a** Alkaline and calcium carbonates, trona (tro) and calcite (cal), coexisting in the same melt inclusion, accompanied by perovskite (prv) and a tabular crystal of phlogopite (phl). **b** Silicate-carbonate inclusion with nepheline (nph) and shortite (sho) associated with calcite (cal), fluorapatite (ap) and perovskite (prv). **c** Melt inclusion containing daughter crystals of sylvite (syl), halite (hl) and pyrochlore (pcl). **d** Calcite (cal) associated with alkaline carbonate (shortite [sho]) in assemblage with perovskite (prv) and cuspidine (csp).

for all reported outcrops. These data suggest that despite their different appearance, the carbonatite lavas from Catanda form a unique carbonatite suite, where all lavas are genetically related and probably originated by pre or post emplacement differentiation from a same original parental magma.

The original composition of the Catanda parental magma has been extrapolated through the study of melt inclusions, which are hosted in the magnetite grains in all the Catanda lava outcrops. Despite the low alkalinity of the Catanda lavas (Supplementary Table A.5) and the low alkali content of their carbonates (Supplementary Table A.1), the daughter mineral assemblage of the magnetite-hosted melt inclusions from all lava locations is made up by primarily sodium- and potassium-rich mineral phases (Fig. 8; Table 2). A similar alkaline melt inclusion association has been described in the intrusive carbonatites from Oka (Canada), in the afrikandites from Kerimasi

(Tanzania), some kimberlite pipes such as Udachnaya-East (Russia) as well as in several carbonatite extrusive localities such as Kerimasi (Tanzania) or the Oldoinyo Lengai volcano (Tanzania) (Chen et al., 2013; Kamenetsky et al., 2007, 2014; Sharygin et al., 2008, 2012; Guzmics et al., 2011, 2012, 2015).

The occurrence of alkaline associations in melt inclusions, formed by phases such as trona, shortite or nyerereite (Table 2) suggest that the formation of Catanda carbonatite lavas was associated with alkali-rich parental magmas.

9.3. Genetic processes

Apart from the melt inclusion evidence and the trachtyoid textures described in the Ipunda lavas, there are other indicators, which support

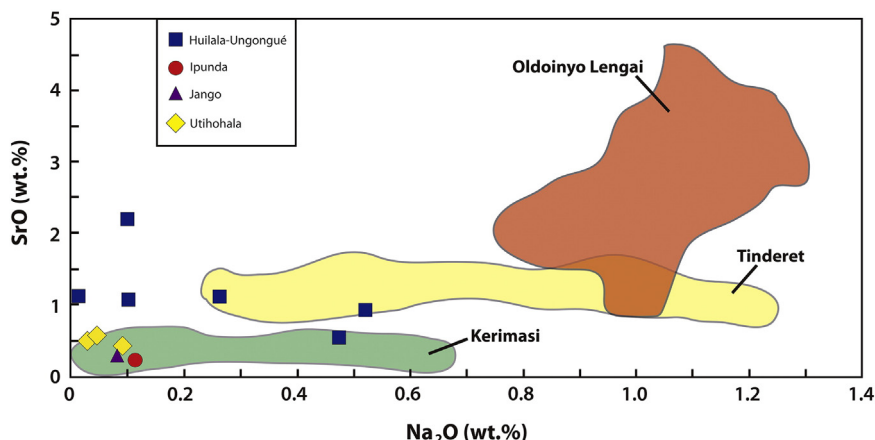


Fig. 9. Catanda carbonates SrO and Na_2O composition compared to natrocarbonatite localities worldwide. Values obtained from Zaitsev et al., 2013.

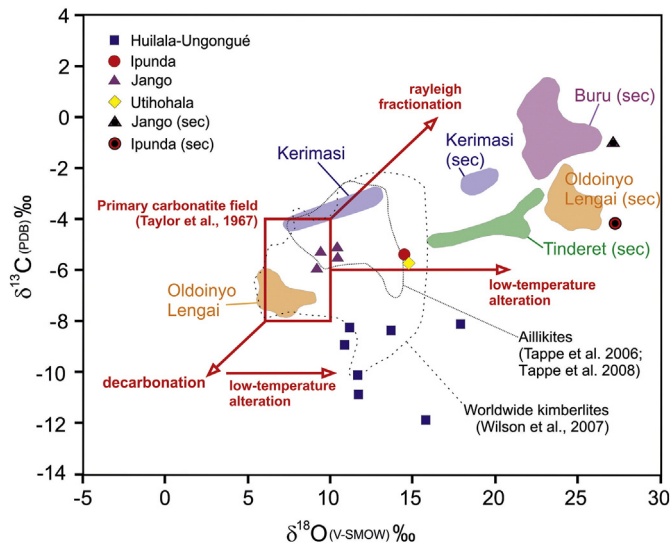


Fig. 10. Graphical comparison of the isotopic composition ($\delta^{13}\text{C}$ and $\delta^{18}\text{O}$) of the Catanda primary and secondary carbonates with the carbonates from other carbonatite and natrocarbonatite localities. Data obtained from Zaitsev et al., 2013. Red arrows indicate trends of isotopic evolution (Demény et al., 2004).

the relation between Catanda extrusive carbonatites and the occurrence of natrocarbonatitic magmatism in the area.

The Sr and Na concentrations of Catanda rock-forming carbonates have been compared with altered natrocarbonatites from Kerimasi and Tinderet, as well with the primary Oldoinyo Lengai natrocarbonatites (Fig. 9). Calcite from Ipunda, Jango and Utihohala, which generally have low Na contents (Supplementary Table A.1), have SrO/Na₂O ratios similar to those reported in the altered natrocarbonatite tephra from the Kerimasi volcano (Zaitsev et al., 2013) indicating that carbonate from these Catanda lavas have equivalent Sr and Na contents to those reported in altered natrocarbonatite localities.

The $\delta^{13}\text{C}$ and $\delta^{18}\text{O}$ signatures of the Catanda magmatic carbonates also present similarities to those reported in altered natrocarbonatites (Fig. 10). The calcicarbonatites from Jango and Utihohala, as well as the altered natrocarbonatite lavas from the Ipunda area exhibit $\delta^{13}\text{C}$ and $\delta^{18}\text{O}$ values between the altered natrocarbonatites from Tinderet and Kerimasi and the primary natrocarbonatites from the Oldoinyo Lengai (Fig. 10). In addition, the secondary sparry calcite analysed in these Catanda localities present similar C and O isotope compositions to those reported in the secondary carbonates from Buru and Oldoinyo Lengai (Zaitsev and Keller, 2006) (Fig. 10). These isotopic relations indicate that calcicarbonatite lavas from Catanda are isotopically comparable to the altered natrocarbonatites worldwide, as well as their secondary sparry carbonates, which have also a similar C and O isotope compositions to those reported in the secondary carbonates analysed in these localities. The evolutionary trend of primary carbonates towards higher oxygen isotope compositions is typically related to fluid alteration processes (Fig. 10) including the alteration of primary alkaline carbonates to calcium rich phases.

On the other hand, silicocarbonatites from the Huilala-Ungongué area do not present evidences of their relation to natrocarbonatite activity. The composition of their groundmass carbonate is significantly enriched in Sr compared to the other Catanda localities and also to the carbonate from altered natrocarbonatites worldwide (Fig. 9). The C and O isotope compositions of the Huilala-Ungongué lavas are significantly different from the other Catanda rocks, presenting similar $\delta^{18}\text{O}$ but lower $\delta^{13}\text{C}$ (Fig. 10). This $\delta^{13}\text{C}$ - $\delta^{18}\text{O}$ relationship defines a significant negative trend (Fig. 10), which may be related to decarbonation processes followed by low-T hydrothermal alteration as has been described in the metacarbonatites of Fuerteventura island (Casillas et al., 2011). Hence, the groundmass of the Huilala-Ungongué silicocarbonatites

contains periclase and calcite, which is a typical mineral association related to the decomposition of dolomite during decarbonation processes (Bucher and Frey, 1994). We hypothesise the formation of these lavas could be due to decarbonation of primary dolomite bearing carbonatites producing the decomposition of dolomite to calcite and periclase forming the typical Huilala-Ungongué groundmass mineral association.

10. Conclusions

1. In Catanda, three types of carbonatitic lavas have been described in four different carbonatite lava outcrops.
2. These three different types of lavas form a unique carbonatite suite, they are genetically related and generated from the same parental melt.
3. The melt inclusion assemblage hosted in magnetite grains is principally formed by alkali-rich phases, arguing for an alkali-rich composition of the Catanda parental melt.
4. Catanda calcicarbonatite lavas present textural, compositional and isotopic features similar to those described in altered natrocarbonatite localities worldwide, such as Tinderet (Kenya) or Kerimasi (Tanzania), which suggest an ancient occurrence of natrocarbonatite lavas in the Catanda area.
5. Silicocarbonatite lavas from the Huilala-Ungongué area present different mineralogical, compositional and isotopic features in comparison to the other Catanda lavas. The $\delta^{13}\text{C}$ - $\delta^{18}\text{O}$ relationship suggests that they were formed in relation to magmatic decarbonation followed by low temperature hydrothermal alteration processes, probably from a primary dolomite bearing carbonatite.

Supplementary data to this article can be found online at <http://dx.doi.org/10.1016/j.lithos.2015.06.016>.

Acknowledgements

This research has been supported by the project CGL2009-13758 of the Spanish Government, the Australian Research Council and the projects SGR-589 and SGR-444 of the Generalitat de Catalunya. Logistics have been also funded by the scholarship program BE-DGR-2012 of the AGAUR (Agència de Gestió d'Ajuts Universitaris i Recerca) and the Hugh E. McKinstry fund, granted by the Society of Economic Geologists (SEG). Assistance during the fieldwork was provided by the Departamento de Geologia da Universidade Agostinho Neto from Luanda, Angola. We thank Joaquín Perona and Xavier Llobet from the Technical Centre of the University of Barcelona (CCiT) for their assistance for the stable isotopes and EPMA analyses respectively. We thank Dr. Paul Davidson (University of Tasmania) for providing informal reviewing and English corrections. We would like to acknowledge the indispensable collaboration and the hospitality during the fieldwork of José Fortuna and Felipe Correia from the village of Catanda. We also thank A. Demény, an anonymous reviewer and associate editor N. Eby for their constructive comments in the article revision.

References

- Bailey, D.K., Kearns, S.L., 2002. High-Ti magnetite in some fine-grained carbonatites and the magmatic implications. *Mineralogical Magazine* 66 (3), 379–384.
- Bambi, A.C.J.M., Costanzo, A., Gonçalves, A.O., Melgarejo, J.C., 2012. Tracing the chemical evolution of primary pyrochlore from plutonic to volcanic carbonatites: the role of fluorine. *Mineralogical Magazine* 76, 393–409.
- Barker, D.S., Nixon, P.H., 1989. High-Ca, low-alkali carbonatite volcanism at Fort Portal, Uganda. *Contributions to Mineralogy and Petrology* 103, 166–177.
- Bell, K., Keller, J., 1995. Carbonatite Volcanism: Oldoinyo Lengai and the Petrogenesis of Natrocarbonatites. 1995. Springer-Verlag, Berlin (210 pp.).
- Bell, K., Simonetti, A., 2010. Source of parental melts to carbonatites - critical isotopic constraints. *Mineralogy and Petrology* 98, 77–89.
- Boctor, N.Z., Boyd, F.R., 1982. Petrology of kimberlite from the DeBruyn and Martin Mine, Bellsbank, South Africa. *Contributions to Mineralogy and Petrology* 76, 253–259.
- Bucher, K., Frey, M., 1994. Petrogenesis of metamorphic rocks. Springer-Verlag, Berlin (318 pp.).

- Calvo, A., Melgarejo, J.C., Bambi, A.C.J.M., Gonçalves, A.O., Alfonso, P., 2011a. Nb and REE at the Bailundo carbonatite, Angola. In: Barra, F. (Ed.), *Let's talk ore deposits*. Universidad Católica del Norte, Antofagasta (Chile), pp. 675–677.
- Calvo, A., Melgarejo, J.C., Alfonso, P., Bambi, A.C.J.M., Gonçalves, A.O., 2011b. Nb and REE mobilization at the Longonjo carbonatite, Angola. In: Barra, F. (Ed.), *Let's talk ore deposits*. Universidad Católica del Norte, Antofagasta (Chile), pp. 681–683.
- Campeny, M., Mangas, J., Melgarejo, J.C., Bambi, A., Alfonso, P., Gernon, T., Manuel, J., 2014. The Catanda extrusive carbonatites (Kwanza Sul, Angola): an example of explosive carbonatitic volcanism. *Bulletin of Volcanology* 76, 818–833.
- Casillas, R., Demény, A., Géza, N., Ahijado, A., Fernández, C., 2011. Metacarbonatites in the Basal Complex of Fuerteventura (Canary Islands). The role of fluid/rock interactions during contact metamorphism and anatexis. *Lithos* 125, 503–520.
- Chakhmouradian, A.R., 2006. High-field-strength elements in carbonatitic rocks: Geochemistry, crystal chemistry and significance for constraining the sources of carbonatites. *Chemical Geology* 235, 138–160.
- Chakhmouradian, A.R., Wall, F., 2012. Rare earth elements: minerals, mines, magnets (and more). *Elements* 8 (5), 333–340.
- Chen, W., Kamenetsky, V.S., Simonetti, A., 2013. Evidence for the alkaline nature of parental carbonatite melts at Oka complex in Canada. *Nature Communications* 4, 2687.
- Church, A.A., 1996. The petrology of the Kerimasi carbonatite volcano and the carbonatites of Oldoinyo Lengai with a review of other occurrences of extrusive carbonatites PhD thesis, University of London (384 pp.).
- Clark, M.G.C., Roberts, B., 1986. Carbonated melilitites and calcitized alkali carbonatites from Homa Mountain, western Kenya: a reinterpretation. *Geological Magazine* 123, 683–692.
- Dalou, C., Koga, T.K., Hammouda, T., Poitras, F., 2009. Trace element partitioning between carbonatitic melts and mantle transition zone minerals: Implications for the source of carbonatites. *Geochimica et Cosmochimica Acta* 73, 239–255.
- Dawson, J.B., 1962a. The geology of Oldoinyo Lengai. *Bulletin of Volcanology* 24, 348–387.
- Dawson, J.B., 1962b. Sodium carbonate lavas from Oldoinyo Lengai, Tanganyika. *Nature* 195, 1075–1076.
- Dawson, J.B., Keller, J., Nyamweru, C., 1995a. Historic and recent eruptive activity of Oldoinyo Lengai. In: Bell, K., Keller, J. (Eds.), *Carbonatite Volcanism. Oldoinyo Lengai and the petrogenesis of natrocarbonatite IAVCEI Proceedings in Volcanology* 4, pp. 4–22.
- Dawson, J.B., Pinkerton, H., Norton, G.E., Pyle, D.M., Browning, P., Jackson, D., Fallick, A.E., 1995b. Petrology and geochemistry of Oldoinyo Lengai lavas extruded in November 1988: magma source, ascent and crystallization. In: Bell, K., Keller, J. (Eds.), *Carbonatite Volcanism. Oldoinyo Lengai and the petrogenesis of natrocarbonatite. IAVCEI Proceedings in Volcanology* 4, pp. 47–69.
- Deans, T., Roberts, B., 1984. Carbonatite tuffs and lava clasts of the Tinderet foothills, western Kenya: a study of calcified natrocarbonatites. *Journal of the Geological Society, London* 141, 563–580.
- Demény, A., Sitnikova, M.A., Karchevsky, P.I., 2004. Stable C and O isotope compositions of carbonatite complexes of the Kola Alkaline Province: phoscorite–carbonatite relationships and source compositions. In: Wall, F., Zaitsev, A.N. (Eds.), *Phoscorites and Carbonatites from Mantle to Mine: the Key Example of the Kola Alkaline Province*. Mineralogical Society, London, pp. 407–431.
- Eby, G.N., Lloyd, F.E., Woolley, A.R., 2009. Geochemistry and petrogenesis of the Fort Portal, Uganda, extrusive carbonatite. *Lithos* 113, 785–800.
- Guzmics, T., Mitchell, R.H., Szabó, C., Berkesi, M., Milke, R., Abart, R., 2011. Carbonatite melt inclusions in coexisting magnetite, apatite and monticellite in Kerimasi caliocarbonatite, Tanzania: melt evolution and petrogenesis. *Contributions to Mineralogy and Petrology* 161, 177–196.
- Guzmics, T., Mitchell, R.H., Szabó, C., Berkesi, M., Milke, R., Ratter, K., 2012. Liquid immiscibility between silicate, carbonate and sulfide melts in melt inclusions hosted in co-precipitated minerals from Kerimasi volcano (Tanzania): evolution of carbonated nephelinitic magma. *Contributions to Mineralogy and Petrology* 164, 101–122.
- Guzmics, T., Zajacz, Z., Mitchell, R.H., Szabó, C., Wälle, M., 2015. The role of liquid–liquid immiscibility and crystal fractionation in the genesis of carbonatite magmas: insights from Kerimasi melt inclusions. *Contributions to Mineralogy and Petrology* 169, 17.
- Habermann, D., Neuser, R.D., Richter, D.K., 1996. REE-activated cathodoluminescence of calcite and dolomite: high-resolution spectrometric analysis of CL emission (HRS-CL). *Sedimentary Geology* 101, 1–7.
- Hay, R.L., 1983. Natrocarbonatite tephra of Kerimasi volcano, Tanzania. *Geology* 11, 599–602.
- Hornig-Kjarsgaard, I., 1998. Rare earth elements in sylvitic carbonatites and their mineral phases. *Journal of Petrology* 39, 2105–2121.
- Issa Filho, A., Dos Santos, A.B.R.M.D., Riffel, B.F., Lapido-Loureiro, F.E.V., McReath, I., 1991. Aspects of the geology, petrology and chemistry of some Angolan carbonatites. *Journal of Geochemical Exploration* 40, 205–226.
- Kamenetsky, V.S., Kamenetsky, M.B., Sharygin, V.V., Golovin, A.V., 2007. Carbonate-chloride enrichment in fresh kimberlites of the Udachnaya-East pipe, Siberia: A clue to physical properties of kimberlite magmas? *Geophysical Research Letters* 34 (9) (L09316).
- Kamenetsky, V.S., Golovin, A.V., Maas, R., Giuliani, A., Kamenetsky, M.B., Weiss, Y., 2014. Towards a new model for kimberlite petrogenesis: Evidence from unaltered kimberlites and mantle minerals. *Earth-Science Reviews* 139, 145–167.
- Keller, J., 1981. Carbonatitic volcanism in the Kaiserstuhl alkaline complex: Evidence for highly fluid carbonatitic melts at the Earth's surface. *Journal of Volcanology and Geothermal Research* 9, 423–431.
- Keller, J., Zaitsev, A.N., 2012. Geochemistry and petrogenetic significance of natrocarbonatites at Oldoinyo Lengai, Tanzania: Composition of lavas from 1988 to 2007. *Lithos* 148, 45–53.
- Korolev, N.M., Marin, Y.B., Nikitina, L.P., Zinchenko, V.N., Chissupa, H.M., 2014. High-Nb Rutile from Upper Mantle Eclogite Xenoliths of the Diamond-Bearing Kimberlite Pipe Catoca (Angola). *Doklady Akademii Nauk* 454 (2), 207–210.
- Le Maitre, R.W., 2002. *Igneous Rocks: a Classification and Glossary of Terms*. Cambridge University Press, Cambridge, U.K.
- Longerich, H.P., Jackson, S.E., Gunther, D., 1996. Laser ablation inductively coupled plasma mass spectrometry transient signal data acquisition and analyte concentration calculation. *Journal of Analytical Atomic Spectrometry* 11, 899–904.
- Mariano, A.N., Roedder, P.L., 1983. Kerimasi: a neglected carbonatite volcano. *Journal of Geology* 91, 449–453.
- McCrea, J.M., 1950. On the Isotopic Chemistry of Carbonates and a Paleotemperature Scale. *Journal of Chemical Physics* 18 (6), 849–857.
- Melgarejo, J.C., Costanzo, A., Bambi, A.C.J.M., Gonçalves, A.O., Neto, A.B., 2012. Subsolidus processes as a key factor on the distribution of Nb species in plutonic carbonatites: The Tchivira case, Angola. *Lithos* 152, 187–201.
- Mitchell, R.H., 1986. *Kimberlites: Mineralogy, Geochemistry and Petrology*. Plenum, New York (442 pp.).
- Mitchell, R.H., Kamenetsky, V.S., 2012. Trace element geochemistry of nyerereite and gregoryite phenocrysts from natrocarbonatite lava, Oldoinyo Lengai, Tanzania: Implications for magma mixing. *Lithos* 152, 56–65.
- Nixon, P.H., Hornung, G., 1973. The carbonatite lavas and tuffs near Fort Portal, western Uganda. *Overseas Geology and Mineral Resources* 41. Institute of Geological Sciences, London, pp. 168–179.
- Pearce, N.J.G., Perkins, W.T., Westgate, J.A., Gorton, M.P., Jackson, S.E., Neal, C.R., Chenery, S.P., 1997. A compilation of new and published major and trace element data for NIST SRM and NIST SRM glass reference materials. *Geostandards Newsletter* 21, 115–144.
- Peres, A.M., Gomes, C.F., Cardoso-Simões, M.V., 1968. As variedades semi-preciosas de olivina da Catanda-Angola. *Boletim dos Serviços de Geologia e Minas de Angola* 18, 5–15.
- Pichou, J.L., Pichou, F., 1984. A new model for quantitative X-ray microanalysis. Part I: application to the analysis of homogeneous samples. *La Recherche Aérospatiale* 3, 13–38.
- Reguir, E.P., Chakhmouradian, A.R., Halden, N., Panseok, Y., Zaitsev, A.N., 2008. Early magmatic and reaction-induced trends in magnetite from the carbonatites of Kerimasi, Tanzania. *Canadian Mineralogist* 46 (4), 879–900.
- Riley, T.R., Bailey, D.K., Lloyd, F.E., 1996. Extrusive carbonatite from the Quaternary Rockeskyll Complex, West Eifel, Germany. *Canadian Mineralogist* 34, 389–401.
- Robles-Cruz, S.E., Escayola, M., Jackson, S., Galí, S., Pervov, V., Watangua, M., Gonçalves, A., Melgarejo, J.C., 2012. U–Pb SHRIMP geochronology of zircon from the Catoca kimberlite, Angola: Implications for diamond exploration. *Chemical Geology* 310–311, 137–147.
- Rozova, Y.V., Frantsesson, E.V., Pleshakov, A.P., Botova, M.M., Filipova, L.P., 1982. High iron chrome spinels in kimberlites of Yakutia. *International Geology Review* 24, 1417–1425.
- Sharygin, V.V., Kamenetsky, V.S., Kamenetsky, M.B., 2008. Potassium sulfides in kimberlite-hosted chloride–nyerereite and chloride clasts of Udachnaya-East Pipe, Yakutia, Russia. *Canadian Mineralogist* 46, 1079–1095.
- Sharygin, V.V., Kamenetsky, V.S., Zaitsev, A.N., Kamenetsky, M.B., 2012. Silicate–natrocarbonatite liquid immiscibility in 1917 eruption combeite–wollastonite nephelinitic, Oldoinyo Lengai Volcano, Tanzania: Melt inclusion study. *Lithos* 152, 23–39.
- Silva, M.V.S., Pereira, E., 1973. Estrutura Vulcânica-Carbonatítica da Catanda (Angola). *Boletim dos Serviços de Geologia e Minas de Angola* 24, 5–14.
- Sun, S., McDonough, W.F., 1989. Chemical and isotopic systematics of oceanic basalts: implications for mantle composition and processes. In: Saunders, A.D., Norry, M.J. (Eds.), *Magmatism in the oceanic basins*. Geological Society of London, Spec. Publ. 42, pp. 313–345.
- Tappe, S., Foley, S.F., Jenner, G.A., Heaman, L.M., Kjarsgaard, B.A., Romer, R.L., Stracke, A., Joyce, N., Hoefs, J., 2006. Genesis of ultramafic lamprophyres and carbonatites at Aillik Bay, Labrador: a consequence of incipient lithospheric thinning beneath the North Atlantic Craton. *Journal of Petrology* 47 (7), 1261–1315.
- Tappe, S., Steinfeldt, A., Heaman, L.M., Simonetti, A., 2009. The newly discovered Jurassic Tikusaq carbonatite–aillikite occurrence, West Greenland, and some remarks on carbonatite–kimberlite relationships. *Lithos* 112S, 385–399.
- Torquato, J.R., Amaral, G., 1973. Algumas idades K/Ar do magmatismo mesozóico de Angola e sua correlação com o correspondente do sul do Brasil. *Boletim do Instituto de Investigação Científica de Angola* 10, 31–38.
- Torró, L., Villanova, C., Castillo, M., Campeny, M., Gonçalves, A.O., Melgarejo, J.C., 2012. Niobium and rare earth minerals from the Virulundo carbonatite, Namibe, Angola. *Mineralogical Magazine* 76, 393–409.
- von Knorring, O., Du Bois, C.G.B., 1961. Carbonatitic lava from Fort Portal area in western Uganda. *Nature* 192, 1064–1065.
- Wallace, M.E., Green, D.H., 1988. An experimental determination of primary carbonatite magma composition. *Nature* 335, 343–346.
- Woolley, A.R., 2001. *Alkaline rocks and carbonatites of the world. Part 3: Africa*. Geological Society of London, London (372 pp.).
- Woolley, A.R., Church, A.A., 2005. Extrusive carbonatites: A brief review. *Lithos* 85, 1–14.
- Woolley, A.R., Kjarsgaard, B.A., 2008. Carbonatites of the world: map and database. *Mineralogical Magazine* 71, 718.
- Zaitsev, A.N., Keller, J., 2006. Mineralogical and chemical transformation of Oldoinyo Lengai natrocarbonatites, Tanzania. *Lithos* 91, 191–207.
- Zaitsev, A.N., Wenzel, T., Venneman, T., Markl, G., 2013. Tinderet volcano, Kenya: an altered natrocarbonatite locality? *Mineralogical Magazine* 77 (3), 213–226.

Table A1

Sample	Huilala - Ungongué								Ipunda		Jango			Utihohala
	AC-19	AC-20	AC-21	AC-24	AC-25	AC-35	AC-36	AC-38	AC-18	AC-39	AC-40	AC-41	AC-17	
<i>ppm</i>														
Na	3524	773.9	3886.2	1944.9	765.8	294.7	109.9	2.7	836.1	233.1	327.7	683.9	606.1	
K	2970.3	597.5	851.4	2188.7	5485.6	49.6	59.3	0,0	104.3	49.4	110.8	129.8	183.9	
Rb	49.2	36.4	16.6	12	375.1	0	0.2	0	0.9	0.1	0.2	0.4	0.4	
Sr	4764.3	9096.6	8067.9	9563.4	18758.5	4759.1	9355.7	210.1	2103.6	4230.3	5168.8	3754.9	2820.1	
Y	97.1	9.2	129.1	22.4	0.9	59.6	14.6	0.3	0.2	0.3	15.8	33.4	0.1	
Nb	346.9	8.2	489.9	70.4	0.1	0.1	35,0	2.0	0.2	0.1	23.1	477.9	0	
Mo	66.9	0.9	8.8	1.1	0.3	0	0.6	0	0.4	0	0.1	0.3	0.1	
Cd	0.3	0.1	0.6	0.1	3.1	0.1	0.1	0	0	0	0	0	0	
Ba	1282.2	3076.4	1639.7	6326.2	2082.6	269	627.4	11.5	6335.3	3479.7	1444.9	933.7	4217.6	
La	763.4	19.7	1190.8	98.5	6.9	333.4	124.6	0.9	0.3	3.5	153.3	268.7	0.4	
Ce	1130.9	30.6	2087.9	174.2	7.2	661.9	203.5	1.5	0.3	2.1	244.9	568.5	0.4	
Pr	100.3	3.6	205.4	18.2	0.7	74,0	23.2	0.1	0	0.4	31.1	62.7	0,0	
Nd	322.4	14.9	717.5	67.7	2.4	283.4	83.4	0.3	0.1	1.6	116.7	242.8	0.1	
Sm	44.7	2.6	93.3	10.8	0.3	40,0	11.4	0	0	0.2	16.1	34.6	0	
Eu	11.9	0.9	24.1	3	0.1	10.7	3.0	0	0.1	0.1	4.7	8.6	0	
Gd	32.2	2.2	62.3	8.7	0.2	27,0	7.2	0	0	0.2	9.9	21.3	0	
Tb	3.7	0.3	6.4	0.9	0	3	0.8	0	0	0	0.9	2.0	0	
Dy	19.4	1.5	30.7	4.8	0.1	13.6	3.6	0	0	0.1	3.8	8.8	0	
Ho	3.4	0.2	4.9	0.8	0	2.2	0.6	0	0	0	0.5	1.3	0	
Er	8.3	0.7	11.4	2	0.1	4.9	1.3	0	0	0	1.2	2.9	0	
Tm	1	0.1	1.2	2	0	0.5	0.1	0	0	0	0.1	0.3	0	
Yb	6.5	0.7	7.2	1.5	0	3.1	0.9	0	0	0	0.8	1.7	0	
Lu	0.9	0.1	0.9	0.2	0	0.4	0.1	0	0	0	0.1	0.2	0	
Hf	4	0.6	5.3	2.4	0	0	0	0	0	0	0.1	7.3	0	
Ta	7.4	0.3	19.7	2.9	0	0	0.3	0	0	0	0.8	21.2	0	
Pb	15.5	3.9	30.3	0.1	4.7	0.8	2.8	0.4	0.2	0	5.2	5.4	0	
Th	7.4	0	62	1.7	0.1	0.4	3.2	0	0	0	3.0	31.6	0	
U	9.9	0.6	17	9.6	0	0	1.3	0.1	0	0	0.3	11.6	0	

Table A2

Sample	Huilala-Ungongué					Ipunda					Jango					Utihohala				
	CAT-10a	CAT-10b	CAT-11a	CAT-11b	CAT-11c	CAT-79a	CAT-79b	CAT-79c	CAT-79c	CAT-79c	AC-39a	AC-39a	AC-41a	AC-41b	AC-41b	AC-17a	AC-17a	AC-17b	AC-17c	AC-17d
<i>wt.%</i>																				
SiO ₂	0.07	0.08	0.11	0.38	0.03	0.04	0.04	0.08	0	0.07	0.01	0.09	0.09	0.09	0.11	0.08	0.15	0.32	0.05	0.11
TiO ₂	14.35	9.25	15.29	8.51	12.83	6.49	11.33	9.99	8.94	12.11	5.36	12.23	7.97	12.87	7.03	11.87	5.09	7.86	13.08	12.02
Al ₂ O ₃	7.24	5.84	5.86	13.06	7.77	5.38	4.53	5.78	3.05	3.16	8.98	3.18	9.65	6.8	8.1	4.14	10.82	14.28	3.87	8.26
Cr ₂ O ₃	0.02	0.01	0.04	0.02	0.04	0.05	0.06	0.06	0.08	0.12	0	0.07	0.03	0.03	0	0.06	0.05	0.04	0.02	0.01
Fe ₂ O ₃	37.53	48.42	34.62	42.84	40.2	53.6	45.46	46.81	50.85	44.04	52.46	44.19	47.51	40.69	50.47	44.45	50.56	42.47	43.59	41.56
FeO	29.64	26.9	38.29	20.92	28.55	25.86	30.16	26.77	29.71	34.27	22.29	32.8	22.06	30.09	23.32	31.12	21.81	20.97	29.03	25.35
V ₂ O ₃	0.05	0	0.17	0	0.02	0.05	0.08	0.03	0.09	0.14	0.03	0.17	0	0	0.02	0.08	0.06	0.02	0.01	0.04
MnO	1.16	1.58	0.6	2.15	1.21	1.31	1.16	1.51	1.1	0.71	1.58	0.94	2.07	0.93	2.53	1.12	1.73	1.57	2.14	2.63
MgO	9.59	7.96	4.85	12.08	9.46	6.94	7.14	8.4	5.76	5.06	8.74	5.95	10.36	8.61	8.59	6.87	9.12	11.99	8.2	10.28
ZnO	0.11	0.04	0.03	0.08	0.11	0.17	0.16	0.09	0.1	0.1	0.17	0.1	0.13	0.11	0.15	0.02	0.13	0.19	0.19	0.08
Total	99.76	100.09	99.86	100.04	100.22	99.9	100.12	99.51	99.67	99.77	99.63	99.72	99.87	100.22	100.32	99.82	99.52	99.71	100.18	100.35
<i>ppm</i>																				
Si	0.002	0.003	0.004	0.013	0.001	0.001	0.002	0.003	0	0.002	0	0.003	0.003	0.003	0.004	0.003	0.005	0.01	0.002	0.004
Ti	0.369	0.242	0.408	0.209	0.328	0.172	0.3	0.262	0.243	0.329	0.139	0.33	0.202	0.333	0.181	0.316	0.13	0.193	0.344	0.305
Al	0.797	0.74	0.745	0.503	0.311	0.274	0.188	0.238	0.13	0.134	0.364	0.134	0.383	0.275	0.327	0.173	0.433	0.549	0.16	0.328
Cr	0.001	0	0.001	0.001	0.001	0.001	0.002	0.002	0.002	0.003	0	0.002	0.001	0.001	0	0.002	0.001	0.001	0.001	0
Fe ³⁺	0.965	1.27	0.925	1.053	1.029	1.425	1.205	1.23	1.381	1.196	1.357	1.193	1.205	1.052	1.302	1.185	1.293	1.043	1.148	1.054
Fe ²⁺	0.847	0.781	1.137	0.572	0.812	0.764	0.888	0.781	0.897	1.035	0.641	0.984	0.622	0.865	0.669	0.922	0.62	0.572	0.849	0.715
V	0.001	0	0.005	0	0.001	0.001	0.002	0.001	0.002	0.004	0.001	0.005	0	0	0.001	0.002	0.002	0.001	0	0.001
Mn	0.034	0.047	0.018	0.06	0.035	0.039	0.035	0.045	0.034	0.027	0.046	0.028	0.059	0.027	0.073	0.033	0.05	0.043	0.063	0.075
Mg	0.488	0.414	0.257	0.588	0.48	0.366	0.375	0.437	0.31	0.272	0.448	0.318	0.521	0.441	0.439	0.363	0.462	0.583	0.428	0.517
Zn	0.003	0.001	0.001	0.002	0.003	0.004	0.004	0.002	0.003	0.003	0.004	0.003	0.003	0.003	0.004	0.001	0.003	0.005	0.005	0.002

Table A3

		Huilala-Ungongué								Ipuanda								Jango								Uihohala							
Sample wt.%		CAT11-51	CAT11-52	CAT11-54	CAT11-59	CAT11-62	CAT179-34	CAT179-35	CAT179-36	CAT179-40	CAT179-43	CAT39-05	CAT39-07	CAT39-08	CAT39-10	CAT39-11	CAT75-67	CAT75-68	CAT75-69	CAT75-70	CAT75-71												
SiO ₂	0.65	0.74	0.68	1.36	0.99	0.99	0.35	1.33	0.43	0.45	0.55	0.6	1.83	1.78	0.5	0.11	1.26	0.84	1.44	2.42	1.26												
MnO	0	0.04	0.13	0.04	0	0	0	0	0.03	0	0.1	0.06	0.05	0	0.01	0.12	0.06	0.02	0	0.07	0.06												
CaO	56.25	55.74	56.06	55.81	55.99	55.98	55.63	55.78	56.01	55.98	56.11	55.76	55.12	55.28	55.11	55.15	55.64	56.27	56.15	55.67	55.98												
Na ₂ O	0.19	0.14	0.2	0.14	0.22	0.16	0.16	0.29	0.27	0.23	0.25	0.28	0.31	0.3	0.24	0.24	0.32	0.22	0.24	0.26	0.26												
P ₂ O ₅	41.31	41.69	41.42	40.09	40.68	42.31	40.29	42.2	42.21	41.86	41.32	39.7	39.88	42.05	42.47	39.73	40.54	39.6	38.02	39.88													
La ₂ O ₃	0.13	0.18	0.07	0	0.18	0.08	0.08	0.13	0	0.15	0.22	0.1	0.28	0.26	0.11	0.03	0.08	0.09	0.07	0.32	0.14												
Ce-O ₃	0.35	0.28	0.24	0.35	0.29	0.27	0.36	0.25	0.21	0.14	0.14	0.27	0.62	0.49	0.39	0.2	0.28	0.18	0.29	0.74	0.26												
SrO	0.37	0.33	0.38	0.34	0.46	0.43	0.43	0.35	0.45	0.37	0.35	0.52	0.46	0.45	0.51	0.52	0.41	0.31	0.33	0.51	0.43												
F	1.37	1.61	1.5	1.14	1.32	1.7	0.98	1.71	1.15	1.5	1.5	1.57	1.06	1.09	1.81	1.95	0.87	1.34	1.25	1.05	1.12												
Cl	0.03	0.04	0	0.05	0.05	0.1	0.09	0.06	0.08	0.09	0.1	0.1	0.06	0.09	0.05	0.11	0.12	0.13	0.13	0.11	0.1												
H ₂ O	1.14	1.03	1.08	1.22	1.15	0.97	1.29	0.98	1.24	1.07	1.02	1.02	1.26	1.24	0.92	0.84	1.32	1.11	1.14	1.23	1.22												
O=F	0.58	0.68	0.63	0.48	0.56	0.71	0.41	0.72	0.49	0.63	0.66	0.45	0.46	0.46	0.76	0.82	0.37	0.56	0.53	0.44	0.47												
O=Cl	0.01	0	0	0.01	0.01	0.02	0.02	0.01	0.02	0.02	0.02	0.02	0.01	0.02	0.01	0.02	0.03	0.03	0.03	0.02	0.02												
Total	101.2	101.13	101.14	100.05	100.77	101.26	100.46	101.65	101.57	101.57	101.57	100.92	100.29	100.39	100.93	100.89	99.69	100.45	100.11	99.94	100.22												
app																																	
Si	0.108	0.123	0.114	0.229	0.166	0.058	0.224	0.071	0.074	0.074	0.091	0.101	0.31	0.301	0.083	0.018	0.214	0.141	0.244	0.413	0.213												
Mn	0	0.005	0.019	0.006	0	0	0	0.004	0	0	0.014	0.009	0.007	0	0.001	0.017	0.009	0.003	0	0.011	0.009												
Ca	10.067	9.951	10.025	10.106	10.078	9.904	10.065	9.944	9.941	9.984	10.008	10.008	9.985	9.993	9.851	9.852	10.138	10.162	10.198	10.204	10.154												
Na	0.061	0.047	0.065	0.045	0.071	0.052	0.094	0.087	0.074	0.079	0.079	0.091	0.102	0.099	0.077	0.077	0.106	0.072	0.078	0.088	0.086												
P	5.842	5.88	5.852	5.736	5.786	5.952	5.744	5.92	5.922	5.886	5.86	5.86	5.683	5.697	5.939	5.994	5.72	5.785	5.683	5.506	5.715												
La	0.008	0.011	0.004	0	0.011	0.005	0.008	0	0.009	0.013	0.006	0.006	0.017	0.016	0.007	0.002	0.005	0.005	0.005	0.002	0.009												
Ce	0.021	0.017	0.015	0.022	0.018	0.017	0.022	0.015	0.013	0.008	0.017	0.017	0.038	0.03	0.024	0.012	0.017	0.011	0.018	0.046	0.016												
Sr	0.036	0.032	0.037	0.033	0.045	0.042	0.042	0.043	0.035	0.034	0.05	0.046	0.045	0.045	0.05	0.05	0.04	0.033	0.033	0.051	0.042												
F	0.725	0.848	0.793	0.61	0.7	0.892	0.523	0.898	0.605	0.786	0.832	0.565	0.581	0.956	1.03	0.469	0.713	0.669	0.566	0.597	0.597												
Cl	0.007	0.01	0.001	0.015	0.013	0.027	0.025	0.016	0.023	0.024	0.029	0.018	0.018	0.025	0.015	0.031	0.034	0.036	0.038	0.031	0.028												
OH	1.267	1.141	1.206	1.375	1.286	1.08	1.452	1.085	1.371	1.19	1.139	1.139	1.416	1.395	1.029	0.939	1.498	1.251	1.293	1.403	1.375												

Table A4

	Huilala-Ungongué							Ipunda			Jango			Utihohala	
Sample wt. %	CAT-10	CAT-10	CAT-10	CAT-11	CAT-11	CAT-11	CAT-11	CAT-79	CAT-79	CAT-79	AC-38	AC-38	AC-39	AC-17	AC-17
SiO ₂	35.93	35.07	36.48	35.98	35.88	35.14	35.90	38.79	36.79	36.22	36.45	36.67	38.51	38.53	36.29
TiO ₂	4.2	1.19	4.05	1.46	1.95	1.38	1.61	2.25	1.17	1.75	1.33	1.62	1.57	1.28	1.50
Al ₂ O ₃	16.91	15.46	16.91	15.31	16.65	15.31	15.36	14.25	15.9	15.88	15.56	16.01	15.22	14.29	15.66
FeO	10.54	10.32	10.33	20.20	19.16	19.76	19.66	9.53	18.1	20.99	19.06	19.21	19.73	19.51	18.60
MnO	0.09	0.32	0.09	0.49	0.44	0.35	0.34	0.16	0.45	0.34	0.46	0.41	0.37	0.40	0.39
MgO	17.43	19.59	17.62	11.07	10.88	10.50	10.90	18.88	11.72	9.66	11.82	11.40	10.53	10.35	10.84
CaO	0.01	0.22	0.09	0.03	0.02	0.06	0.02	0.83	0.08	0.08	0.04	0.03	0.06	0.05	0.06
Na ₂ O	0.58	0.07	0.47	0.22	0.29	0.36	0.25	0.37	0.14	0.33	0.21	0.15	0.26	0.25	0.38
K ₂ O	0.62	10.24	9.56	9.87	10.01	8.74	9.98	5.90	9.97	9.95	9.88	9.96	9.43	9.38	9.88
SrO	0.01	0	0	0	0	0	0	0	0	0	0	0	0	0	0
BaO	0.39	0.39	0.38	0.16	0.19	0.04	0.12	0.21	0.08	0.22	0.06	0.15	0.04	0.05	0.15
ZnO	0.02	0.09	0.02	0.09	0.13	0.10	0.07	0.04	0.09	0.06	0.02	0.17	0	0.09	0
F	0.2	0.34	0.22	0.32	0.31	0.33	0.26	0.23	0.33	0.16	0.47	0.47	0.30	0.27	0.35
Cr ₂ O ₃	0.05	0.07	0.07	0.11	0.05	0.08	0.09	0.16	0.21	0.21	0.03	0.15	0.14	0.12	0.05
NiO	0	0.01	0.03	0.01	0	0.04	0	0.05	0	0	0.05	0.01	0.02	0.01	0
Li ₂ O	0.76	0.51	0.92	0.78	0.75	0.53	0.75	1.58	1.01	0.84	0.91	0.97	1.50	1.51	0.86
H ₂ O*	4.03	3.81	4.06	3.76	3.81	3.65	3.77	4	3.81	3.86	3.73	3.77	3.90	3.87	3.74
Subtotal	100.75	97.68	101.3	99.86	100.51	97.37	99.09	97.24	99.84	100.53	100.07	101.14	101.59	99.94	98.74
O/F	0.08	0.14	0.09	0.13	0.13	0.14	0.11	0.10	0.14	0.07	0.20	0.20	0.13	0.11	0.15
Total	100.67	97.54	101.21	99.73	100.38	97.23	98.98	97.14	99.70	100.46	99.87	100.94	101.46	99.83	98.59
Si	5.22	5.30	5.26	5.52	5.44	5.53	5.53	5.65	5.56	5.53	5.54	5.51	5.71	5.81	5.58
Al iv	2.78	2.70	2.74	2.48	2.56	2.47	2.47	2.35	2.44	2.47	2.46	2.49	2.29	2.19	2.42
Al vi	0.12	0.06	0.13	0.29	0.41	0.37	0.33	0.10	0.42	0.38	0.32	0.35	0.37	0.35	0.41
Ti	0.46	0.13	0.44	0.17	0.22	0.16	0.19	0.25	0.13	0.20	0.15	0.18	0.17	0.15	0.17
Cr	0.01	0.01	0.01	0.01	0.01	0.01	0.01	0.02	0.03	0.02	0	0.02	0.02	0.01	0.01
Fe	1.28	1.30	1.25	2.59	2.43	2.60	2.54	1.16	2.28	2.68	2.42	2.42	2.45	2.46	2.39
Mn	0.01	0.04	0.01	0.06	0.06	0.05	0.04	0.02	0.06	0.04	0.06	0.05	0.05	0.05	0.05
Mg	3.77	4.41	3.78	2.53	2.46	2.46	2.51	4.10	2.64	2.20	2.68	2.55	2.33	2.33	2.48
Zn	0	0.01	0	0.01	0.01	0.01	0.01	0	0.01	0.01	0	0.02	0	0.01	0
Ni	0	0	0	0	0	0	0	0.01	0	0	0.01	0	0	0	0
Li*	0.44	0.31	0.53	0.48	0.45	0.34	0.47	0.93	0.61	0.52	0.55	0.59	0.90	0.91	0.53
Ca	0	0.04	0.01	0.01	0.0	0.01	0	0.13	0.01	0.01	0.01	0	0.01	0.01	0.01
Na	0.16	0.02	0.13	0.07	0.09	0.11	0.08	0.11	0.04	0.1	0.06	0.04	0.08	0.07	0.11
K	1.78	1.98	1.76	1.93	1.94	1.96	1.96	1.10	1.92	1.94	1.91	1.91	1.78	1.80	1.84
Sr	0	0	0	0	0	0	0	0	0	0	0	0	0	0	0
Ba	0.02	0.02	0.02	0.01	0.01	0	0.01	0.01	0	0.01	0	0.01	0	0	0.01
OH*	3.91	3.84	3.90	3.85	3.85	3.83	3.87	3.89	3.84	3.92	3.78	3.78	3.86	3.87	3.83
F	0.09	0.16	0.10	0.15	0.15	0.17	0.13	0.11	0.16	0.08	0.22	0.22	0.14	0.13	0.17
TOTAL	20.06	20.34	20.08	20.16	20.09	20.08	20.13	19.93	20.15	20.11	20.18	20.15	20.15	20.16	20.12
Y total	6.09	6.28	6.15	6.15	6.05	6.01	6.08	6.59	6.17	6.05	6.20	6.18	6.28	6.27	6.05
X total	1.97	2.05	1.92	2.01	2.03	2.08	2.05	1.34	1.98	2.06	1.99	1.97	1.87	1.89	2.07
Al total	2.90	2.75	2.87	2.77	2.97	2.84	2.79	2.45	2.85	2.86	2.79	2.84	2.66	2.54	2.84
Fe/Fe+Mg	0.25	0.23	0.25	0.51	0.50	0.51	0.49	0.22	0.46	0.55	0.48	0.49	0.51	0.51	0.49

Table A5

Sample wt. %	Huilala-Ungongué							Ipunda			Jango			Utihohala	
	CAT-10	CAT-10	CAT-10	CAT-11	CAT-11	CAT-11	CAT-11	CAT-79	CAT-79	CAT-79	AC-38	AC-38	AC-39	AC-17	AC-17
SiO ₂	35.93	35.07	36.48	35.98	35.88	35.14	35.90	38.79	36.79	36.22	36.45	36.67	38.51	38.53	36.29
TiO ₂	4.2	1.19	4.05	1.46	1.95	1.38	1.61	2.25	1.17	1.75	1.33	1.62	1.57	1.28	1.50
Al ₂ O ₃	16.91	15.46	16.91	15.31	16.65	15.31	15.36	14.25	15.9	15.88	15.56	16.01	15.22	14.29	15.66
FeO	10.54	10.32	10.33	20.20	19.16	19.76	19.66	9.53	18.1	20.99	19.06	19.21	19.73	19.51	18.60
MnO	0.09	0.32	0.09	0.49	0.44	0.35	0.34	0.16	0.45	0.34	0.46	0.41	0.37	0.40	0.39
MgO	17.43	19.59	17.62	11.07	10.88	10.50	10.90	18.88	11.72	9.66	11.82	11.40	10.53	10.35	10.84
CaO	0.01	0.22	0.09	0.03	0.02	0.06	0.02	0.83	0.08	0.08	0.04	0.03	0.06	0.05	0.06
Na ₂ O	0.58	0.07	0.47	0.22	0.29	0.36	0.25	0.37	0.14	0.33	0.21	0.15	0.26	0.25	0.38
K ₂ O	0.62	10.24	9.56	9.87	10.01	8.74	9.98	5.90	9.97	9.95	9.88	9.96	9.43	9.38	9.88
SrO	0.01	0	0	0	0	0	0	0	0	0	0	0	0	0	0
BaO	0.39	0.39	0.38	0.16	0.19	0.04	0.12	0.21	0.08	0.22	0.06	0.15	0.04	0.05	0.15
ZnO	0.02	0.09	0.02	0.09	0.13	0.10	0.07	0.04	0.09	0.06	0.02	0.17	0	0.09	0
F	0.02	0.34	0.22	0.32	0.31	0.33	0.26	0.23	0.33	0.16	0.47	0.47	0.30	0.27	0.35
Cr ₂ O ₃	0.05	0.07	0.07	0.11	0.05	0.08	0.09	0.16	0.21	0.21	0.03	0.15	0.14	0.12	0.05
NiO	0	0.01	0.03	0.01	0	0.04	0	0.05	0	0	0.05	0.01	0.02	0.01	0
Li ₂ O	0.76	0.51	0.92	0.78	0.75	0.53	0.75	1.58	1.01	0.84	0.91	0.97	1.50	1.51	0.86
H ₂ O*	4.03	3.81	4.06	3.76	3.81	3.65	3.77	4	3.81	3.86	3.73	3.77	3.90	3.87	3.74
Subtotal	100.75	97.68	101.3	99.86	100.51	97.37	99.09	97.24	99.84	100.53	100.07	101.14	101.59	99.94	98.74
O/F	0.08	0.14	0.09	0.13	0.13	0.14	0.11	0.10	0.14	0.07	0.20	0.20	0.13	0.11	0.15
Total	100.67	97.54	101.21	99.73	100.38	97.23	98.98	97.14	99.70	100.46	99.87	100.94	101.46	99.83	98.59
Si	5.22	5.30	5.26	5.52	5.44	5.53	5.53	5.65	5.56	5.53	5.54	5.51	5.71	5.81	5.58
Al iv	2.78	2.70	2.74	2.48	2.56	2.47	2.47	2.35	2.44	2.47	2.46	2.49	2.29	2.19	2.42
Al vi	0.12	0.06	0.13	0.29	0.41	0.37	0.33	0.10	0.42	0.38	0.32	0.35	0.37	0.35	0.41
Ti	0.46	0.13	0.44	0.17	0.22	0.16	0.19	0.25	0.13	0.20	0.15	0.18	0.17	0.15	0.17
Cr	0.01	0.01	0.01	0.01	0.01	0.01	0.01	0.02	0.03	0.02	0	0.02	0.02	0.01	0.01
Fe	1.28	1.30	1.25	2.59	2.43	2.60	2.54	1.16	2.28	2.68	2.42	2.42	2.45	2.46	2.39
Mn	0.01	0.04	0.01	0.06	0.06	0.05	0.04	0.02	0.06	0.04	0.06	0.05	0.05	0.05	0.05
Mg	3.77	4.41	3.78	2.53	2.46	2.46	2.51	4.10	2.64	2.20	2.68	2.55	2.33	2.33	2.48
Zn	0	0.01	0	0.01	0.01	0.01	0.01	0	0.01	0.01	0	0.02	0	0.01	0
Ni	0	0	0	0	0	0	0	0.01	0	0	0.01	0	0	0	0
Li*	0.44	0.31	0.53	0.48	0.45	0.34	0.47	0.93	0.61	0.52	0.55	0.59	0.90	0.91	0.53
Ca	0	0.04	0.01	0.01	0.0	0.01	0	0.13	0.01	0.01	0.01	0	0.01	0.01	0.01
Na	0.16	0.02	0.13	0.07	0.09	0.11	0.08	0.11	0.04	0.1	0.06	0.04	0.08	0.07	0.11
K	1.78	1.98	1.76	1.93	1.94	1.96	1.96	1.10	1.92	1.94	1.91	1.91	1.78	1.80	1.84
Sr	0	0	0	0	0	0	0	0	0	0	0	0	0	0	0
Ba	0.02	0.02	0.02	0.01	0.01	0	0.01	0.01	0	0.01	0	0.01	0	0	0.01
OH*	3.91	3.84	3.90	3.85	3.85	3.83	3.87	3.89	3.84	3.92	3.78	3.78	3.86	3.87	3.83
F	0.09	0.16	0.10	0.15	0.15	0.17	0.13	0.11	0.16	0.08	0.22	0.22	0.14	0.13	0.17
TOTAL	20.06	20.34	20.08	20.16	20.09	20.08	20.13	19.93	20.15	20.11	20.18	20.15	20.15	20.16	20.12
Y total	6.09	6.28	6.15	6.15	6.05	6.01	6.08	6.59	6.17	6.05	6.20	6.18	6.28	6.27	6.05
X total	1.97	2.05	1.92	2.01	2.03	2.08	2.05	1.34	1.98	2.06	1.99	1.97	1.87	1.89	2.07
Al total	2.90	2.75	2.87	2.77	2.97	2.84	2.79	2.45	2.85	2.86	2.79	2.84	2.66	2.54	2.84
Fe/Fe+Mg	0.25	0.23	0.25	0.51	0.50	0.51	0.49	0.22	0.46	0.55	0.48	0.49	0.51	0.51	0.49

Table A6

Sample	Primary carbonate											Secondary carbonate		Travertine	
	Huilala - Ungongué							Ipunda	Jango			Utihohala		Jango	Ipunda
	AC-19	AC-20	AC-21	AC-24	AC-25	AC-35	AC-36	CAT-79	AC-39	AC-41	AC-42	AC-17	AC-42s	CAT-79s	AC-01t
δ ¹³ C (V-PDB)	-10.97	-8.93	-8.38	-10.18	-8.11	-8.31	-12.15	-5.49	-5.34	-5.53	-5.2	-5.61	-1.02	-4.15	6.37
δ ¹⁸ O (V-SMOW)	11.66	10.66	13.44	11.58	17.85	11.02	15.79	14.33	9.33	10.35	10.29	14.5	26.95	27.2	26.42